AD_____

Award Number: W81XWH-08-1-0492

TITLE: Evaluating Surgical Margins with Optical Spectroscopy and Spectral Imaging Following Breast Cancer Resection

PRINCIPAL INVESTIGATOR: Matthew D. Keller

CONTRACTING ORGANIZATION: Vanderbilt University
Nashville, TN 37235

REPORT DATE: August 2009

TYPE OF REPORT: Annual Summary

PREPARED FOR: U.S. Army Medical Research and Materiel Command
Fort Detrick, Maryland 21702-5012

REPORT DOCUMENTATION PAGE

Form Approved
OMB No. 0704-0188

1. REPORT DATE *(DD-MM-YYYY)*	**2. REPORT TYPE**	**3. DATES COVERED** *(From - To)*
01-08-2009	annual summary	1 Aug 2008 - 31 July 2009

4. TITLE AND SUBTITLE
Evaluating Surgical Margins with Optical Spectroscopy and

Spectral Imaging Following Breast Cancer Resection

5a. CONTRACT NUMBER
W81XWH-08-1-0492

5b. GRANT NUMBER
BC083203

5c. PROGRAM ELEMENT NUMBER

6. AUTHOR(S)
Matthew D. Keller

Email: matthew.d.keller@vanderbilt.edu

5d. PROJECT NUMBER

5e. TASK NUMBER

5f. WORK UNIT NUMBER

7. PERFORMING ORGANIZATION NAME(S) AND ADDRESS(ES)

Vanderbilt University
Nashville, TN 37235

8. PERFORMING ORGANIZATION REPORT NUMBER

9. SPONSORING / MONITORING AGENCY NAME(S) AND ADDRESS(ES)
CDMRP BCRP
U.S. Army Medical Research and Materiel Command
Fort Detrick, MD 21702-5012

10. SPONSOR/MONITOR'S ACRONYM(S)

11. SPONSOR/MONITOR'S REPORT NUMBER(S)

12. DISTRIBUTION / AVAILABILITY STATEMENT
Approved for public release; distribution unlimited

13. SUPPLEMENTARY NOTES

14. ABSTRACT
In one aspect of the fellowship, a training program has been established to expose the PI to a wide range of current breast cancer research, particularly through seminars in imaging and cancer biology fields. Collaborations with other graduate students and mentoring of undergraduate students has also been pursued. In the research portion, polarized fluorescence and reflectance-based imaging was initially pursued to examine breast tumor surgical margin status intraoperatively during breast conserving therapy. After achieving insufficient results, the approach was modified to spatially offset Raman spectroscopy (SORS) to achieve the proper depth sampling needed for the clinical procedure. Results thus far have shown the feasibility of the SORS approach for detecting breast tumor signatures under up to 2 millimeters of normal breast tissue. Efforts are currently underway to develop a Monte Carlo simulation model to further understand the results. Two full-length manuscripts, several conference talks, and a BCRP Idea Award have all grown from this work.

15. SUBJECT TERMS
fluorescence, reflectance, spatially offset Raman spectroscopy, surgical margin evaluation, Monte Carlo modeling, therapeutic guidance, partial mastectomy, breast conserving therapy

16. SECURITY CLASSIFICATION OF:			**17. LIMITATION OF ABSTRACT**	**18. NUMBER OF PAGES**	**19a. NAME OF RESPONSIBLE PERSON**
a. REPORT	**b. ABSTRACT**	**c. THIS PAGE**			USAMRMC
U	U	U	UU	61	**19b. TELEPHONE NUMBER** *(include area code)*

Table of Contents

Page

Introduction

For the training portion of this fellowship, the plan included attending and presenting research at a number of relevant seminars and national conferences and working closely with my mentor and collaborators in a variety of fields related to breast cancer research. The result of this program is that I will be a well-rounded research scientist with knowledge of basic science, translational research, and clinical research as they relate to breast cancer. I will have a solid foundation of skills needed to achieve his career goals as an investigator in a highly collaborative environment thanks to the extensive education, experience, and interaction with others built in to this program and the proposed research.

For the research aspect of this fellowship, the primary goal is to improve the intraoperative evaluation of surgical margin status during partial mastectomies for breast cancer treatment. For many of the approximately 180,000 women diagnosed with early-stage invasive breast cancer or carcinoma *in situ* each year [1], a viable treatment option is breast conserving therapy (BCT). BCT involves a partial mastectomy, or lumpectomy, to remove only the primary lesion with a small amount of surrounding normal tissue [2]. Depending on the hospital, the depth of normal tissue required from the surgical margin on the excised specimen to the tumor is typically 1-2 millimeters [3]. If tumor-positive margins are found, a second operation is necessary because positive margins are a major predictor of local tumor recurrence [4]. Currently available intraoperative margin evaluation tools all have significant drawbacks [5-7], so there is a need for an automated, real-time method to accurately evaluate surgical margins during BCT.

Light-based methods have the potential to provide automated, fast determination of surgical margin status in the operating room during the surgery without disrupting or removing any tissue for such analysis. Fluorescence and diffuse reflectance spectroscopy have been researched extensively as a diagnostic tool for identifying suspicious lesions and detecting the presence of malignancy in the breast [8-10]. Rather than using small fiber optic probes, fluorescence and reflectance-based spectral imaging, in which fluorescence and reflectance spectra are recorded for each pixel in an image, is a more viable method for a surgical guidance tool. Prior studies in non-imaging modalities [11] also showed promise that adding polarization optics to a spectral imaging system would enhance the depth information from these modalities so that margins could be evaluated to the required depth of at least 1 mm. Thus the proposed work was to develop the use of polarized fluorescence and reflectance-based imaging first in a laboratory setting and then in a clinical setting.

Body

The following is the original statement of work for the training portion of this fellowship.

Task 1. Provide a training program to prepare the PI for a successful career as a breast cancer researcher (months 1-24).

A. attend relevant seminars and journal clubs through the Biomedical Engineering department, the VU Institute of Imaging Science (VUIIS), and the VU Medical Center (months 1-24)
B. work with the mentor on learning all about the various methods of optically characterizing breast tissue (months 1-24)
C. work with clinical collaborator to learn about new developments in diagnosing breast cancer and monitoring therapy for it (months 1-24)
D. meet with Ph.D. committee to track progress and gain new perspectives on the project from faculty doing research on various aspects of breast cancer (months 1-24)
E. watch for any highly relevant courses on breast cancer to audit (months 1-24)
F. work with other graduate students doing different kinds of research related to breast cancer and doing similar research in other organ systems (months 1-24)
G. mentor undergraduate students learning to do basic aspects of research (months 1-24)
H. attend national conferences in both biomedical optics and breast cancer to present the proposed research (months 10-24)
I. present research at the seminars listed above (months 13-24)

Work Completed in Year 1

This training program has been followed mostly as outlined. More specifics for each sub-task above are as follows:

A. I have attended several seminars relevant to breast cancer research, primarily related to improving imaging modalities such as MRI for detecting breast cancer through VUIIS. I have also attended seminars on disparities (racial, socioeconomic, etc.) in breast cancer treatment and on novel molecular targets for breast cancer detection/treatment.
B. My current research has required greater optical characterization knowledge than I had from previous classes and research, so in conjunction with my advisor, I have learned a great deal about determining and exploiting various optical properties (scattering, absorption, anisotropy, etc.) of breast tissues.
C. This has been accomplished via periodic meetings with the two primary surgical oncologists with whom we do research. Topics have included trends in choosing partial vs. total mastectomies, attitudes about other novel margin assessment techniques being pursued, and the possibility of expanding the current research to examine lymph node status as an off-shoot project.
D. A meeting with committee members was held ~6 months after this fellowship was awarded, in which I apprised them of my progress and we discussed how best to proceed with various optical techniques.
E. No such relevant courses were found in Year 1.

F. I have worked with several other graduate stu dents using optica l m eans f or simila r projects. In particular, I have provided data processing assistance to the student working on using fluorescence and reflectance-based im aging for brain tum or delineation, and I have assisted in m ost aspects on a project using fluorescence to intraoperatively detect the presence of parathyroid glands to prevent their accidental removal.
G. Several undergraduate student s had summ er internships in m y lab, and I provided assistance to several of them – prim arily for growing cell cultu res and im proving data processing procedures.
H. I have presented m y research at nu merous major conferences, including *SPIE Photonics West, European Conferences on Biomedical Optics*, and was an invited speaker at two stops in a research symposium series sponsored by ThermoFisher Scientific.
I. N/A for Year 1.

The following is the original sta tement of work for the research phase, aim ed at developing the use of polarized fluorescence and reflectance spectral im aging as a real-tim e m ethod for evaluating surgical margins during breast tumor resection.

Task (1): **Validate the ability of polarized spectral imaging to provide depth-dependant information in a lab setting, with both tissue phantoms and breast tissue samples (months 1-6).**

A. determine appropriate optical properties of normal and tumor breast tissue from literature (month 1)
B. construct tissue phantoms from gelatin, hemoglobin, polystyrene microspheres, and fluorescent dyes, and measure their optical properties – repeat as necessary until phantoms very closely match the optical properties of breast tissue (months 1-2)
C. take polarized spectral images of phantoms simulating various relevant biological tissue distributions, such as "tumor" tissue underlying a small layer of "fat" tissue (months 3-4)
D. analyze spectral line shapes from image regions known to have different properties, especially in the z direction, to ensure that changing polarization angle provides depth-dependant information while maintaining other spectral features (months 3-4)
E. acquire human breast tissue samples from tissue bank – use benchtop SI system to measure these samples and ones already available in the PI's lab for a total of about 30 samples (month 5)
F. analyze these polarized spectra (relative to histopathology report) with MRDF and SMLR to assess the ability of polarized SI to detect pathology that standard spectroscopy cannot (months 5-6)

Work Completed During Year 1

Sub-tasks A-D above were com pleted to the fulle st extent possible. Optical properties for normal breast vs. breast tum or tissues were obtained, and appropriate phantom s were developed. Polarized spectral images of these phantoms were obtained as well, bu t at this point it was clear that a problem had been encountered. Figure 1 show s the results from Majumder et al. (a former post-doc in the PI's lab) for using polarized fluorescence spectroscopy on a layered phantom of

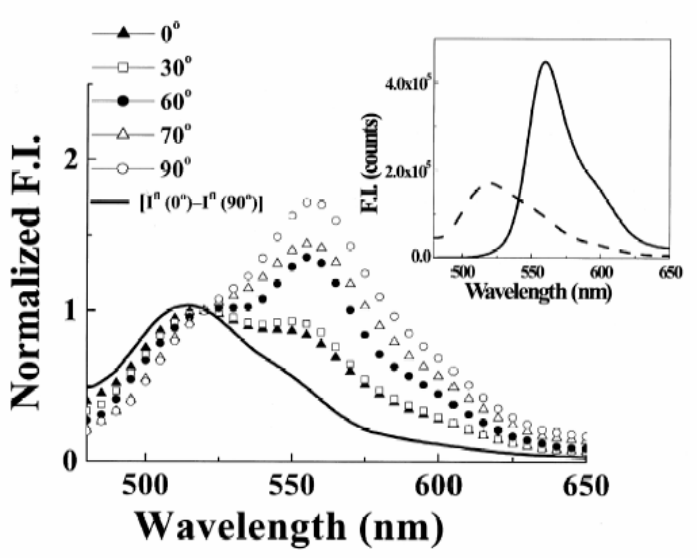

Figure 1 Fluorescence spectra showing relative contributions of riboflavin (520 nm) and rhodamine (560 nm) for layered phantom as the angle between excitation and detection leg polarizers changes (legend in upper left).

riboflavin (peak at 520 nm) over rhodam ine (peak at 560 nm), with each layer also includ ing polystyrene m icrospheres to act as optical scat terers. One can see that changing the relative angle between the polarizers in the excitation and detection legs produced dram atic effects for the relative contributions from the top and bottom layers. Howe ver, when identical ph antoms were used in polarized fluorescence i maging mode (rather than single-point spectroscopy), the best results obtained are shown in Figure 2. Despite much effort, no greater layer discrim ination could be achieved with this phantom or with other fluorophores / scatterers. Using phantom s

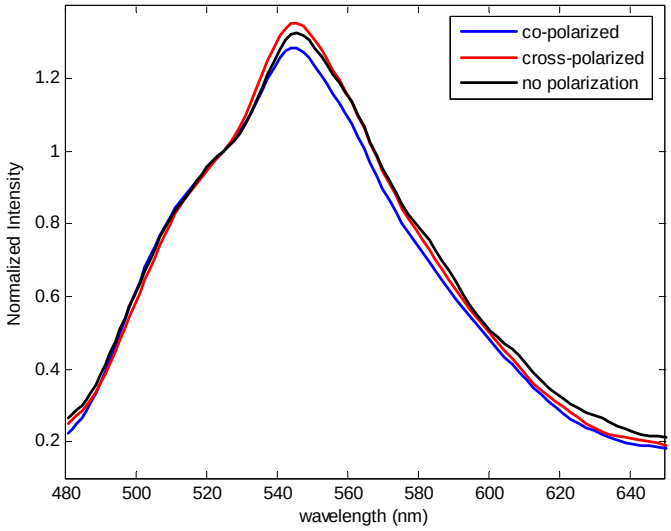

Figure 2 Spectra obtained from phantoms constructed in same manner as in Fig 1, but in imaging, rather than single-point mode. Co-polarized = 0 degrees, Cross- = 90 degrees.

with optical properties similar to those of tissues, it was also determined that this technique was not gathering information from far enough below the surface to be clinically useful in breast tumor surgical margin analysis. A likely reason for this disparity is the finding that spectra obtained from point vs. imaging mode have fundamental lineshape differences due to the typical path traveled by photons in each modality [12].

Task (2): Acquire polarized spectral images from a large population of lumpectomy cases to develop discrimination algorithms and compare with point spectroscopy results (months 7-24).

A. obtain approval for study from Vanderbilt IRB, VICC SRC, and USAMRMC (prior to month 7)
B. obtain co- and cross-polarized spectral images and probe-based spectra of excised breast tissues in the OR from a minimum of 30 patients (months 7-16)
C. correlate interrogated regions of breast tissue with histopathology (months 7-16)
D. process and normalize spectra from images and probe – build a database of all spectra (months 7-16)
E. use MRDF and SMLR to develop a discrimination algorithm for separating normal and tumor breast tissues on the basis of all spectra available (month 17)
F. apply discrimination algorithm to all pixels in previously obtained spectral images to test its accuracy (months 17-18)
G. continue to obtain polarized spectral images and apply discrimination algorithm prospectively – correlate results with histopathology (months 19-24)

Work Completed During Year 1

The portions of sub-tasks A-E *not* involving polarized spectral images were completed. That is, probe-based spectra were obtained from freshly excised breast tissues in the operating room, correlated with histology / margin status, and a discrimination algorithm was developed to classify the spectra. In one case, a set of non-polarized spectral images was obtained as well to act as an initial test of the feasibility of using spectral imaging in general. These results are detailed in a copy of the manuscript written about that work ("Autofluorescence and diffuse reflectance spectroscopy and spectral imaging for breast surgical margin analysis"), which is included in the Appendix of this report.

Revising the Research Plan

Since it appeared that polarized spectral imaging was not the optimal solution for intraoperative breast tumor surgical margin evaluation, a new optical approach capable of the needed depth sampling was sought. Several groups have successfully applied Raman spectroscopy (a type of inelastic light scattering that probes the biochemical content of a substance) for cancer diagnosis, primarily in epithelial tissues [13] because of the limited depth from which typical Raman setups can gather significant signal. The most practical and promising method for detecting signals from deeper tissues, at least 1 mm below the surface, is introducing

a spatial offset between the delivery and collection fibers in a technique known as spatially offset Raman spectroscopy (SORS) [14].

In SORS, larger offsets are more likely to detect photons that have traveled deeper into tissue via multiple scattering, compared with smaller separations, which detect superficial photons that have only undergone minimal scattering events. Matousek et al. first demonstrated SORS of diffusely scattering media using a two-layer chemical phantom [14]. To date, the primary biological application of this technique has been detecting the strong Raman signature of bone through several millimeters of soft tissue [15-17]. It has also been used to detect the Raman spectral features of hydroxyapatite crystals (found in breast calcifications) through overlying lean chicken breast tissue [18]. Thus, the application of SORS had been limited to detecting very strong scatterers with unique spectral features under a layer of generic soft tissue. No work had, to our knowledge, yet been published in applying SORS to discriminating multiple layers of soft tissue. An initial feasibility test was performed by creating a phantom with a 1 mm thick layer of chicken fat tissue (akin to normal human, fatty breast tissue) over a piece of lean chicken meat (a more fibrous, denser tissue, as are most tumors). Raman spectra were acquired at a number of source-detector offsets. As shown in Figure 3, increasing this offset resulted in spectra losing features of the fat layer and gaining features of the muscle layer.

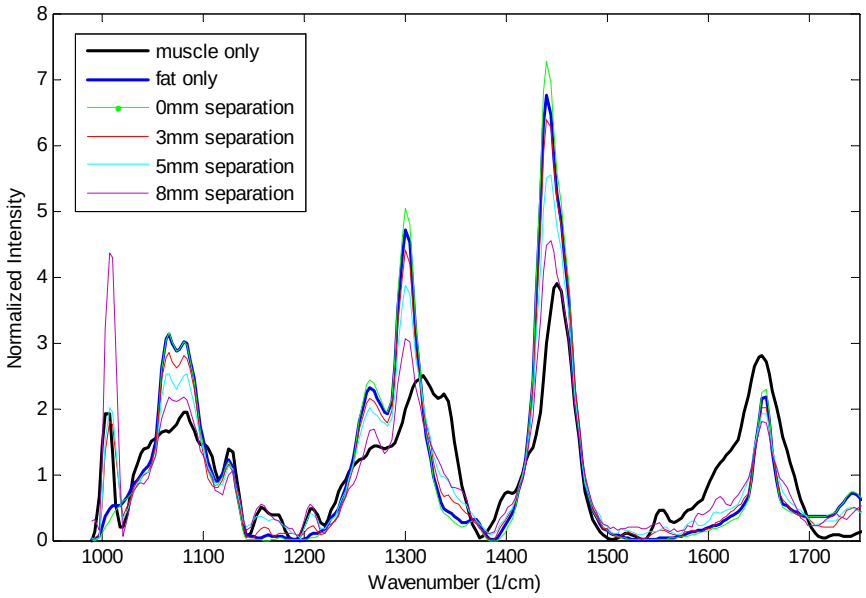

Figure 3: SORS spectra at various offsets for fat over muscle phantom.

Given the success of the initial feasibility study, tissue constructs were made with layers of normal human breast tissue, between two very thin quartz coverslips, overlying human breast tumor samples. Normal layer thicknesses of 0.5, 1, and 2 mm were achieved by placing appropriate spacers between the coverslips. These thicknesses were chosen to represent the clinical margin standards and to include a thinner layer as a positive control. These normal layers were placed directly on top of invasive breast cancer tissue samples. SORS measurements were then made at a number of source-detector offsets. Full details of this work can be found in the manuscript "Spatially Offset Raman Spectroscopy of Layered Soft Tissues" in the Appendix. In short, the results showed that it is possible to detect the presence of breast tumors under up to

2mm of normal tissue, as needed for clinical margin analysis. This work also raised questions about the detection limits of SORS for this application; i.e. how small of a tumor layer can be detected under how thick of a top normal layer.

To answer these questions, a numerical simulation model is the desired approach. In particular, Monte Carlo simulations are a ubiquitous probability-based method to track the paths of photons according to tissue optical properties. Since examining numerous combinations of precisely controlled layer thicknesses is not practical experimentally, these simulations would be extremely useful in the design of a multi-separation SORS probe to be used for margin analysis in the clinic.

Revised Statement of Work

Given the lack of expected results with polarized fluorescence and reflectance imaging and the success with SORS measurements, the remainder of this fellowship's research aspect will be focused on developing SORS for breast tumor surgical margin analysis. [Note that the SOW begins at month 5, to reflect the approximate time point of beginning SORS work, and ends at month 18, the PI's expected graduation date].

Task 1: Characterize the relationship between source-detector separation and depth of interrogation in spatially offset Raman spectroscopy (SORS) of breast tissues.

A. Design and construct a simple SORS setup with components available in the PI's lab (Month 5)
B. Design tissue models that mimic a multi-layer soft tissue, such as normal and malignant breast tissues. (Months 5-6)
C. Characterize the relationship between source-detector separation and depth interrogated using the tissue model (Month 7)
D. Repeat above steps with breast tissue samples (Months 8-9)
E. Identify the parameters such as S-D separation, signal strength, integration times, etc. needed to interrogate such tissues to a depth of 1-2 mm (Month 10)

Task 2: Model the relationship between source-detector separation and depth of interrogation in spatially offset Raman spectroscopy (SORS) of breast tissues.

A. Develop reliable Monte Carlo model capable of simulating SORS measurements (Months 11-12)
B. Validate model by comparing to experimental results obtained in Task 1 (Month 13)
C. Use model to examine effect of coverslip layers in Task 1 (Month 13)
D. Perform simulations for a wide range of normal layer and tumor layer thicknesses to examine probable minimum detection limits (Month 14)
E. Same as D, but with other tissue layers included, such as an additional normal layer under the tumor layer (Month 14)

Task 3: Design and test a SORS probe for evaluating margin status in the operating room.

A. Using results from Task 2, design a fiber optic-based SORS probe with multiple source-detector separations to interrogate breast tissue up to the clinically relevant 2 mm depth (Month 15)
B. Test SORS probe with layered tissue constructs to ensure its depth performance (Month 15)
C. Use probe to btain spectra from heterogeneous breast tissue samples *ex vivo* to validate this approach in intact tissue specimens rather than in layered constructs. (Month 16)
D. Perform a small pilot study to use SORS for evaluating margin status in the to ensure this technique's applicability in such an environment (Months 17-18).

By completing these tasks, the use of SORS for intraoperative breast tumor surgical margin analysis is expected to be validated and well-characterized. While the technique is not the one originally proposed, the end result will be equivalent.

Work Completed During Year 1

As discussed above, Task 1 has been completed. For Task 2, the Monte Carlo model has been completed, although no formal results are yet available to display.

Key Research Accomplishments

- Confirmed ability of combined autofluorescence and diffuse reflectance spectroscopy (and non-polarized spectral imaging) to discriminate normal versus malignant breast tissues at the surgical margin on freshly excised specimens from partial mastectomies
- Showed that polarized fluorescence imaging cannot provide the depth enhancement seen in point-based polarized fluorescence spectroscopy
- Demonstrated the feasibility of performing SORS on layered soft tissues
- Characterized relationship between source-detector offset and relative spectral contributions from each layer for normal breast tissue overlying breast tumors
- Developed Monte Carlo code with sufficient detail to be a true Raman Monte Carlo code also capable of tracking photons in a manner needed for SORS measurements

Key Training Accomplishments

- Attended numerous seminars related to breast cancer research outside of my narrow field
- Presented research at a number of conferences both in the US and in Europe
- Used input of Ph.D. committee to reshape goals

Reportable Outcomes

Peer-reviewed journal articles:

Keller MD, Majumder SK, Kelley MC, Meszoely I, Boulos FI, Olivares GM, and Mahadevan-Jansen A. Autofluorescence and Diffuse Reflectance Spectroscopy and Spectral Imaging for Surgical Margin Evaluation during Breast Cancer Resection. *Lasers Surg Med* (in review).

Keller MD, Majumder SK, and Mahadevan-Jansen A. Spatially offset Raman spectroscopy of layered soft tissues. *Opt Lett* 34(7), 926-928, 2009.

Conference Proceedings and Presentations:

Keller MD, Kelley MC, Mahadevan-Jansen A. Depth-resolved measurements in breast tissues with spatially offset Raman spectroscopy. Presented at: *SPIE Photonics West*, Advanced Biomedical and Clinical Diagnostic Systems VII, 2009.

Keller MD and Mahadevan-Jansen A. Spatially offset Raman spectroscopy for breast surgical margin evaluation. In: *European Conferences on Biomedical Optics*, Clinical and Preclinical Tissue Characterization I, ThE2, 2009.

Keller MD and Mahadevan-Jansen A. Spatially offset Raman spectroscopy for breast surgical margin evaluation. Presented at: ThermoFisher Research Symposium, 2009. (Invited Talk)

Keller MD and Mahadevan-Jansen A. Spatially Offset Raman spectroscopy for soft tissue cancers. Presented at: *FACSS Annual Meeting* (upcoming), 2009. (Invited Talk)

Research Funding Received:

Department of Defense Breast Cancer Research Program Idea Award (W81XWH-09-1-0037)
Spatially offset Raman spectroscopy for margin evaluation during breast conserving therapy
1/1/09 to 12/31/11
$375,000
The objective of this project is to develop the use of spatially offset Raman spectroscopy as a tool to improve intraoperative margin evaluation to ensure complete tumor removal with negative margins during breast conserving therapy.

Conclusions

The training program has been a very valuable experience so far. It has ensured that I hear about current research related to breast cancer that I may not otherwise know about within my own field of research. This has given me a more well-rounded background to help in my future career as a breast cancer investigator.

In the research program, there was much promise in the planned approach of doing polarized spectral imaging for margin analysis; however, results strongly indicate that such an approach was not destined for a successful application for breast tumor surgical margin analysis. Instead, I have pioneered the use of SORS for examining layered soft tissues, in particular normal breast over breast tumors. Results thus far have shown the ability to detect breast tumor signatures under up to 2 mm of normal tissue, and have drawn much interest from the scientific and medical communities. The further development of a Monte Carlo code should enable an even deeper understanding of the use of SORS for this application, and that knowledge will then be used in the near future to design a SORS probe to use in actual surgical margin evaluation.

References

1. American Cancer Society, "Cancer Facts and Figures 2009," (American Cancer Society, Atlanta, 2009).

2. K. I. Bland, and E. M. C. III, eds. *The Breast: Comprehensive Management of Benign and Malignant Disorders* (Saunders, St. Louis, 2004).

3. A. Taghian, M. Mohiuddin, R. Jagsi, S. Goldberg, E. Ceilley, and S. Powell, "Current perceptions regarding surgical margin status after breast-conserving therapy: results of a survey," Annals of surgery **241**, 629-639 (2005).

4. K. C. Horst, M. C. Smitt, D. R. Goffinet, and R. W. Carlson, "Predictors of local recurrence after breast-conservation therapy," Clin Breast Cancer **5**, 425-438 (2005).

5. E. K. Valdes, S. K. Boolbol, I. Ali, S. M. Feldman, and J. M. Cohen, "Intraoperative touch preparation cytology for margin assessment in breast-conservation surgery: does it work for lobular carcinoma?," Ann Surg Oncol **14**, 2940-2945 (2007).

6. T. P. Olson, J. Harter, A. Munoz, D. M. Mahvi, and T. Breslin, "Frozen section analysis for intraoperative margin assessment during breast-conserving surgery results in low rates of re-excision and local recurrence," Ann Surg Oncol **14**, 2953-2960 (2007).

7. G. C. Balch, S. K. Mithani, J. F. Simpson, and M. C. Kelley, "Accuracy of intraoperative gross examination of surgical margin status in women undergoing partial mastectomy for breast malignancy," Am Surg **71**, 22-27; discussion 27-28 (2005).

8. C. Zhu, T. M. Breslin, J. Harter, and N. Ramanujam, "Model based and empirical spectral analysis for the diagnosis of breast cancer," Optics express **16**, 14961-14978 (2008).

9. Z. Volynskaya, A. S. Haka, K. L. Bechtel, M. Fitzmaurice, R. Shenk, N. Wang, J. Nazemi, R. R. Dasari, and M. S. Feld, "Diagnosing breast cancer using diffuse reflectance spectroscopy and intrinsic fluorescence spectroscopy," Journal of Biomedical Optics **13**, 024012-024019 (2008).

10. S. K. Majumder, M. D. Keller, F. I. Boulos, M. C. Kelley, and A. Mahadevan-Jansen, "Comparison of autofluorescence, diffuse reflectance, and Raman spectroscopy for breast tissue discrimination," J Biomed Opt **13**, 054009 (2008).

11. N. Ghosh, S. K. Majumder, H. S. Patel, and P. K. Gupta, "Depth-resolved fluorescence measurement in a layered turbid medium by polarized fluorescence spectroscopy," Opt Lett **30**, 162-164 (2005).

12. S. C. Gebhart, S. K. Majumder, and A. Mahadevan-Jansen, "Comparison of spectral variation from spectroscopy to spectral imaging," Appl Opt **46**, 1343-1360 (2007).

13. M. D. Keller, E. M. Kanter, and A. Maha devan-Jansen, "Raman spectroscopy for cancer diagnosis," Spectroscopy **21**, 33-41 (2006).

14. P. Matousek, I. P. Clark, E. R. Dr aper, M. D. Morris, A. E. Goodship, N. Everall, M. Towrie, W. F. Finney, and A. W. Parker, "Subsurface probing in diffusely scattering media using spatially offset Raman spectroscopy," Appl Spectrosc **59**, 393-400 (2005).

15. P. Matousek, E. R. Draper, A. E. Goodship, I. P. Clark, K. L. Ronayne, and A. W. Parker, "Noninvasive Raman spectroscopy of human tissue in vivo," Appl Spectrosc **60**, 758-763 (2006).

16. M. V. Schulm erich, K. A. Dooley, M. D. Mo rris, T. M. Vanasse, and S. A. Goldstein, "Transcutaneous fiber optic Ram an spectrosc opy of bone using annular illum ination and a circular array of collection fibers," Journal of biomedical optics **11**, 060502 (2006).

17. N. A. Macleod, A. Goodship, A. W. Parker, and P. Matousek, "Pre diction of sublayer depth in turbid m edia using spatially offs et R aman spectroscopy," A nalytical chem istry **80**, 8146-8152 (2008).

18. N. Stone, R. Baker, K. Rogers, A. W. Pa rker, and P. Matousek, "Subsurface probing of calcifications with spatially offset Ra man spe ctroscopy (SORS): future possibilities for the diagnosis of breast cancer," Analyst **132**, 899-905 (2007).

Appendices

Appendix 1 – Current Biosketch for Matthew Keller, pages 18 – 20.

Appendix 2 – Manuscript 1: Keller MD**,** Majumder SK, Kelley MC, Meszoely I, Boulos FI, Olivares GM, and Mahadevan-Jansen A. Autofluorescence and Diffuse Reflectance Spectroscopy and Spectral Imaging for Surgical Margin Evaluation during Breast Cancer Resection. *Lasers Surg Med* (in review), pages 21 – 47

Appendix 3 – Manuscript 2: Keller MD, Majumder SK, and Mahadevan-Jansen A. Spatially offset Raman spectroscopy of layered soft tissues. *Opt Lett* 34(7), 926-928, 2009, pages 48 – 61.

BIOGRAPHICAL SKETCH

NAME Matthew David Keller	POSITION TITLE Ph.D. Student

EDUCATION/TRAINING

INSTITUTION AND LOCATION	DEGREE	YEAR(s)	FIELD OF STUDY
Vanderbilt University, Nashville, TN B.E.		2003	Biomedical Engineering
Vanderbilt University, Nashville, TN M.S.		2006	Biomedical Engineering
Vanderbilt University, Nashville, TN	Ph.D.	*exp. 2009*	Biomedical Engineering

Positions and Employment:

2000 Engineering Tech, Missman, Stanley, and Associates, Rock Island, IL
2001 Research Assistant, Argonne National Laboratory, Lemont, IL
2002 Research Assistant, National Institutes of Health, Bethesda, MD
2003 Research Assistant, Northwestern University, Evanston, IL
2003 – present Research Assistant (Ph.D. student), Vanderbilt University, Nashville, TN

Honors & Awards:

Newport Research Excellence Award at SPIE Photonics West, January 2008.
Dissertation enhancement grant, Vanderbilt Graduate School, November 2008.
Tomas Hirschfeld Scholar Award for outstanding submission to FACSS annual meeting, August 2008.
Third place finisher in student debate panel at Gordon Research Conference, July 2008.
Department of Defense Breast Cancer Research Program Predoctoral Fellowship, Summer 2008.
Top Spear Award for high grade in Medical School Physiology class (1st engineer to earn it), Spring 2004.
Howard Hughes Medical Institute Pre-Doctoral Fellowship, awarded April 2003.
Founder's Medal, received for graduating first in class, Vanderbilt University, May 2003.
BMES Rita Schaffer Award, for outstanding leadership, scholarship, and service, awarded Spring 2003.
Barry Goldwater Scholarship, for outstanding promise in scientific research, awarded March 2002.
Dean's List Highest Honors, Vanderbilt University, Fall 1999 to Spring 2003.
Tau Beta Pi (engineering honor society), inducted December 2001.
Full-tuition engineering undergraduate scholarship, Vanderbilt University, 1999 to 2003.

Professional Affiliation:

International Society for Optical Engineering (SPIE) - member
Optical Society of America (OSA) – member
Society for Applied Spectroscopy (SAS) - member

Peer-reviewed Publications:

Keller MD, Kanter EM, and Mahadevan-Jansen A. Raman spectroscopy for cancer diagnosis (cover), *Spectroscopy* 21(11), 33-41, 2006.

Majumder SK, **Keller MD**, Kelley MC, Boulos FI, and Mahadevan-Jansen A. Comparison of autofluorescence, diffuse reflectance, and Raman spectroscopy for breast tissue discrimination. *Journal of Biomedical Optics* 13, 054009, 2008. **NOTE**: functioned as co-first-author on this publication.

Patil CA, Bosschaart N, **Keller MD**, van Leeuwen TG, and Mahadevan-Jansen A. A Combined Raman Spectroscopy – Optical Coherence Tomography Device for Tissue Characterization. *Opt Lett* 33, 1135-1137, 2008.

Keller MD, Kanter EM, Lieber CA, Majumder SK, Hutchings J, Ellis D, Beaven R, Stone N, Mahadevan-Jansen A. Detecting Temporal and Spatial Effects of Epithelial Cancers with Raman Spectroscopy. *Disease Markers* 25(6), 323-337, 2008.

Kanter EM, Vargis E, Majum der SK, **Keller MD**, Kanter GJ, Rao GG, Mahadeva n-Jansen A. Application of Raman Spectroscopy for Cervical Dysplasia Diagnosis. *Journal of Biophotonics* 2(1-2), 81-90, 2009.

Keller MD and Mahadevan-Jansen A. Spatially offset Raman spectroscopy of layered soft tissues. *Opt Lett* 34(7), 926-928, 2009.

Keller MD, Majumder SK, Kelley MC, Meszoely I, Boulos FI, Olivares GM, and Mahadevan-Jansen A. Autofluorescence and Diffuse Reflectance Spectroscopy and Spectral Imaging for Surgical Margin Evaluation during Breast Cancer Resection. *Lasers Surg Med* (in review).

Paras C, **Keller MD**, White L, Phay J, Mahadevan-Jansen A. "Seeing" the Parathyroid During Surgery. *Nature Med* (in review), 2009.

Proceedings Papers (accompanying presentations)**:**

Majumder SK, **Keller MD**, Kelley MC, and Mahadevan-Jansen A. Optical detection of breast tumors - a comparison of diagnostic performance of autofluorescence, diffuse reflectance, and Raman spectroscopy. In: *Proceedings of SPIE* (Vo Dinh T and Cohn G, eds.), **6430C**, 2007.

Keller MD, Majumder SK, Kelley MC, Meszoely I, Boulos FI, and Mahadevan-Jansen A. Optical spectroscopy for therapeutic guidance in breast conserving therapy. In: *Proceedings of SPIE* (Schweitzer D and Fitzmaurice M, eds.), **66280J,** 2007.

Keller MD, Majumder SK, Kelley MC, Meszoely I, Boulos FI, Olivares GM, and Mahadevan-Jansen A. Optical Spectroscopy and Spectral Imaging for Evaluating Surgical Margin Status during Breast Cancer Resection, in Biomedical Optics CD-ROM (The Optical Society of America, Washington, DC, 2008), BSuB6.

Keller MD and Mahadevan-Jansen A. Spatially offset Raman spectroscopy for breast surgical margin evaluation. In: *European Conferences on Biomedical Optics*, Clinical and Preclinical Tissue Characterization I, ThE2, 2009.

Presentations:

Keller MD, Robichaux-Viehoever A, Lieber C, and Mahadevan-Jansen A. Using organotypic raft cultures to understand the biological basis of Raman spectra obtained from normal vs. cancerous skin. Presented at: *SPIE Photonics West*, Vibrational Spectroscopy Conference, 2006.

Keller MD, Majumder SK, Kelley MC, Meszoely I, Boulos FI, Olivares GM, and Mahadevan-Jansen A. Fluorescence and Reflectance Spectroscopy and Spectral Imaging for Evaluating Surgical Margin Status during

Breast Cancer Resection. Presented at: *SPIE Photonics West*, Advanced Biomedical and Clinical Diagnostic Systems VI, 2008.

Keller MD, Majumder SK, Kelley MC, and Mahadevan-Jansen A. Feasibility of using spatially offset Raman spectroscopy (SORS) for evaluating breast surgical margins. Presented at: Gordon Research Conference – Lasers in Medicine and Biology, 2008.

Keller MD and Mahadevan-Jansen A. Spatially Offset Raman Spectroscopy for depth-resolved measurements in excised breast tissues. Presented at: FACSS Annual Meeting, 2008.

Keller MD, Kelley MC, Mahadevan-Jansen A. Depth-resolved measurements in breast tissues with spatially offset Raman spectroscopy. Presented at: *SPIE Photonics West*, Advanced Biomedical and Clinical Diagnostic Systems VII, 2009.

Paras C, **Keller MD**, White L, Phay J, Mahadevan-Jansen A. Optical guidance of endocrine surgery. Presented at: *SPIE Photonics West*, Advanced Biomedical and Clinical Diagnostic Systems VII, 2009.

Keller MD and Mahadevan-Jansen A. Spatially offset Raman spectroscopy for breast surgical margin evaluation. Presented at: Thermo Research Symposium, 2009. (Invited Talk)

Keller MD and Mahadevan-Jansen A. Spatially Offset Raman spectroscopy for soft tissue cancers. Presented at: *FACSS Annual Meeting* (upcoming), 2009. (Invited Talk)

Autofluorescence and diffuse reflectance spectroscopy and spectral imaging for breast surgical margin analysis

Matthew D. Keller, MS,[1] Shovan K. Majumder, PhD,[1,2] Mark C. Kelley, MD,[3] Ingrid M. Meszoely, MD,[3] Fouad I. Boulos, MD,[4] Graciela M. Olivares, MD,[4] and Anita Mahadevan-Jansen, PhD[1*]

[1]Department of Biomedical Engineering, Vanderbilt University, Nashville, Tennessee 37235

[2]Laser Biomedical Applications and Instrumentation Division, Raja Ramanna Centre for Advanced Technology, Indore, India 452 013

[3]Division of Surgical Oncology, Vanderbilt University Medical Center, Nashville, Tennessee 37232

[4]Division of Pathology, Vanderbilt University Medical Center, Nashville, Tennessee 37232

[*]Corresponding author

Keywords: breast cancer, margin assessment, optical diagnosis, therapeutic guidance

ABSTRACT

Background and Objective: Most women with early stage breast cancer have the option of breast conserving therapy, which involves a partial mastectomy for removal of the primary tumor, usually followed by radiotherapy. The presence of tumor at or near the margin is strongly correlated with the risk of local tumor recurrence, so there is a need for a non-invasive, real-time tool to evaluate margin status. This study examined the use of autofluorescence and diffuse reflectance spectroscopy and spectral imaging to evaluate margin status intraoperatively.

Materials and Methods: Spectral measurements were taken from the surface of the tissue mass immediately following removal during partial mastectomies and/or from tissues immediately after sectioning by surgical pathology. A total of 145 normal spectra were obtained from 28 patients, and 34 tumor spectra were obtained from 12 patients.

Results: After correlation with histopathology, a multivariate statistical algorithm classified the spectra as normal (negative margins) or tumor (positive margins) with 85% sensitivity and 96% specificity. A separate algorithm achieved 100% classification between neo-adjuvant chemotherapy-treated tissues and non-treated tissues. Fluorescence and reflectance-based spectral images were able to demarcate a calcified lesion on the surface of a resected specimen as well.

Conclusion: Fluorescence and reflectance spectroscopy could be a valuable tool for examining the superficial margin status of excised breast tumor specimens, particularly in the form of spectral imaging to examine entire margins in a single acquisition.

1. INTRODUCTION

Of the approximately 180,000 patients each year diagnosed with early-stage invasive breast cancer or breast carcinoma *in situ* (1), most have the option of breast conserving therapy (BCT). This method consists of removing the primary breast lesion via a lumpectomy, or partial mastectomy, which is often followed by directed radiotherapy. To be successful, the surgical portion of BCT must ensure that no tumor cells remain within a specified distance of the surgical margin on the removed specimen; this case is described as negative margins. The presence of positive margins is strongly correlated with the risk of local tumor recurrence and necessitates a second operation for the patient (2). The exact size of the negative margin required varies significantly among different hospitals and can range from simply finding no tumor cells on the surface to having > 5 mm between tumor cells and the surface of the specimen (3,4). Some women with tumors considered too large for BCT may elect to have neo-adjuvant chemotherapy (NAC) to shrink the tumor and eliminate the necessity of a total mastectomy (5,6). NAC has also been shown to improve the prognosis following BCT for some groups of women (5,6).

Currently available methods of evaluating margin status intraoperatively include visual inspection of the excised tissue by the surgeon, which is incorrect in at least 25% of cases (7). Frozen section pathology and cytological examination ("touch prep") are commonly used but require tissue to be sent to pathology and are prone to sampling error (7,8). While ultrasound is available in the operating room, its poor spatial resolution results in limited sensitivity (7,9). The current gold standard in margin analysis is serial sectioning with standard histopathology, but results may take several days to over a week. These limitations emphasize the need for a real-time, intraoperative margin evaluation tool that can assure complete removal of breast tumors with negative margins in a single procedure.

Autofluorescence and diffuse reflectance spectroscopy have been researched extensively as a diagnostic tool for discriminating among normal, malignant, and/or benign breast tissues (10-22). Some of the most extensive recent work has been performed by Ramanujam et. al., who have used numerous approaches to discriminate breast tissues with autofluorescence and/or diffuse reflectance, including the use of multiple excitation wavelengths (23,24), multiple source-detector fiber separations (25), and Monte Carlo-based extraction algorithms (26-28). The use of diffuse reflectance as well as intrinsic fluorescence from molecules like collagen and NADH for breast tissue classification was explored by Feld et. al. (29). Most of this work, though, is focused on diagnostic applications rather than on therapeutic guidance. One exception to this comment is a study performed by Bigio et. al. using *in vivo* elastic scattering measurements to both make a diagnosis and help guide resection; they were able to distinguish malignant from normal tissue with sensitivities up to 69% and specificities up to 93% (30).

In a previous *ex vivo* study in our lab, autofluorescence (excited at 337 nm) and diffuse reflectance (400-800 nm) were used to classify breast tissue samples in to four categories: invasive ductal carcinoma (IDC), ductal carcinoma *in situ* (DCIS), fibroadenoma (FA), and normal. Using a multi-class discrimination algorithm with leave-one-sample-out cross-validation, fluorescence only, reflectance only, and combined (concatenated) fluorescence and reflectance classified tissues with 72%, 71%, and 84% accuracies, respectively. The combined approach also had ~ 84% sensitivity and 90% specificity for distinguishing normal/benign tissue from malignant tissues in general (31).

The problem with the above approaches for intraoperative margin analysis is that probing a small area (~1mm diameter) at a time for each measurement on a sample that is typically at least a few centimeters in diameter is not very practical. Fluorescence and diffuse reflectance-

based multi-spectral imaging would be better suited for this application; this approach records reflectance and fluorescence spectra for each pixel in an image. In separate work in our lab, combined fluorescence and reflectance spectroscopy discriminated normal, tumor core, and tumor margin tissues in the brain with a 95% classification rate (32). A multi-spectral imaging system with a 25 mm by 25 mm field of view was then developed, and its use has produced results similar to those obtained with the point spectroscopy system (33).

Based on these past results with breast and brain tissues, the goal of this study was to investigate the use of combined autofluorescence and diffuse reflectance spectroscopy and spectral imaging for evaluating the status of surgical margins intraoperatively during lumpectomies. Point spectra were gathered from freshly excised breast tissue specimens and correlated with histopathology/margin status at the measurement locations. In two cases, spectral images were obtained as well to assess the feasibility of that approach.

2. MATERIALS AND METHODS

2.1 Patient data

Women undergoing breast conserving therapy or, in some cases, total mastectomy, were recruited for this study by the surgical oncologists (MK and IM). Informed consent was obtained under a protocol approved by the Vanderbilt University Institutional Review Board and Vanderbilt-Ingram Cancer Center Scientific Review Committee. Table 1 displays the breakdown of the types of measurements taken, after excluding spectra for which no detailed pathology was available. Spectra were also excluded if they showed drastically altered shapes due to strong absorption by blood (this was minimized by rinsing the tissue with saline) or by a blue dye used to identify sentinel lymph nodes; interference from the blue dye was mostly

eliminated by the surgeons' changing the site of its injection. A total of 145 spectra from clinically normal tissues, indicative of negative margins, from 28 patients were used in the below analysis. A total of 34 such spectra were obtained from tissue sites containing tumors (IDC or DCIS) within ~1mm in depth from the measurement surface, indicative of positive margins, from 12 patients. Eight of the patients had measurements taken from both normal and tumor regions. An average of five to six, minimum of one, and maximum of 12 spectra were used from any one patient; however, the maximum number of spectra from a given tissue type from any one patient was seven. In addition, a total of 19 spectra were obtained from normal regions of three patients who had undergone neo-adjuvant chemotherapy; these spectra were excluded from further analysis except where explicitly noted. Due to the nature of the study population, no measurements were obtained from benign tumors such as fibroadenomas.

2.2 Instrumentation

Autofluorescence and diffuse reflectance spectra of breast tissues were measured using a portable spectroscopic system. A high-pressure nitrogen laser (Spectra Physics, Mountain View, CA) was used as the excitation source for autofluorescence measurements, and a 150-W attungsten-halogen lamp (Ocean Optics, Dunedin, FL) emitting broadband white light from 400 nm to 800 nm was used for diffuse reflectance measurements. Light delivery to and collection from the sample was achieved with a fiber optic probe (Romack, Williamsburg, VA) consisting of seven 300 μm core diameter fibers arranged in a six-around-one configuration. Two of the surrounding fibers delivered laser and white light consecutively to the tissue sample while the remaining fibers collected autofluorescence and diffuse reflectance from the tissue sample. Emissions collected by the fiber optic probe were serially dispersed and detected with a chip -

based spectrometer (Ocean Optics, Dunedin, FL). For autofluorescence measurements, reflected laser light was eliminated with a 365 nm long-pass filter placed in front of the entrance slit of the spectrometer. For this study, the output power of the white light was ~0.6 mW at the tissue surface, and the nitrogen laser was operated at a 20-Hz repetition rate, 5-nanosecond pulse width, and average pulse energy of 45±5 μJ at the tissue surface. An integration time of 100 ms was used for each spectral measurement.

Spectral images were obtained with a liquid-crystal tunable filter (LCTF) spectral imaging system, as previously described (33). Briefly, a Varispec VIS-20 LCTF (CRI, Inc., Woburn, MA) was used to cycle through a user-defined range of detection wavelengths between 400 and 720 nm, and emitted light was collected with a variable focal-length camera lens (f/3.5, Nikon, Tokyo, Japan). Images at each defined wavelength were collected with a thermo-electrically cooled CCD camera (PhotonMax, Princeton Instruments, Princeton, NJ) to create a 3D data cube. Images were acquired in a non-contact manner with a 25 mm by 25 mm field of view and an object distance of 180 mm. A 500 W xenon arc lamp, bandpass filtered at 340 nm, was used for fluorescence excitation, while a 200 W halogen lamp (Luxtec, West Boylston, MA) was used for diffuse reflectance excitation. A 365 nm dichroic filter coupled both illumination sources into a single, 10-mm-core liquid light guide, which delivered the illumination light to the sample.

2.3 Data acquisition

For lumpectomy procedures, autofluorescence and diffuse reflectance spectra were obtained from one point on each of the six facets of the removed specimen as soon as it was resected in the operating room. Additional measurements on the surface were made at times at the surgeon's

discretion. If a large residual tumor was present and time permitted (i.e. it was done within ~30 minutes of removal), or for total mastectomy procedures, measurements were taken after initial gross sectioning of the tissue. Taking such measurements from sections including tumors was necessary to increase the sample size of tumor/positive margin measurements. For spectral imaging, one fluorescence and one reflectance image, along with the corresponding baseline image, were acquired for three of the six margins of the lumpectomy specimen. Total acquisition time for each margin was approximately 60-90 seconds.

In all point spectroscopy cases, the measured spots were marked for correlation with histopathology. For the standard six measurements on lumpectomies described above, surgical sutures were used both to orient the specimen and to indicate the measurement spots. For all other measurements, the spots were marked with a standard tissue dye. The marked spots were sampled by a trained pathologist (FB or GO) via shave biopsies for correlating the spectra with tissue histopathology. All findings were interpreted as they would be for margin analysis - i.e., any measured spots with malignant cells within 1mm of the surface on which the probe was placed were deemed to be tumor/positive margins. Thus, the phrases normal tissue or negative margins, and tumor tissue or positive margins are used interchangeably throughout the text.

2.4 Data processing and analysis

After autofluorescence and diffuse reflectance spectral acquisition, a set of reference spectra from a fluorescence and a reflectance standard were recorded to correct for inter-sample variability due to variations in laser-pulse energy and white light power. The fluorescence standard was a low-concentration Rhodamine 6G solution (2mg/L) contained in a quartz cuvette, and the reflectance standard was a 20 % reflectance plate (Labsphere, North Sutton, NH) placed

in a black box. All subsequent processing and analysis was performed in MATLAB 7.0.1 (Mathworks, Natick, MA). Raw fluorescence and diffuse reflectance spectra were processed to remove instrumentation-induced variations and to yield calibrated spectra, the details of which are described elsewhere (34). Autofluorescence spectra were truncated from 365-650 nm, and diffuse reflectance spectra were truncated from 400-800 nm. The resultant spectra were further corrected for the non-uniform spectral response of the detection system and normalized to the overall integrated intensity to remove the absolute intensity information from the spectra that might be affected by many unavoidable experimental factors.

The processed fluorescence and reflectance spectra were merged prior to analysis with a two-part classification method, which was performed with leave-one-patient-out cross-validation. Maximum representation and discrimination feature (MRDF) was first used to reduce the dimensionality of the data and to extract the relevant diagnostic features. Those output features were then classified by sparse multinomial logistic regression (SMLR), which assigned a posterior probability of the measured spectrum belonging to each of the tissue classes. The spectrum was assigned to the category for which it had the highest probability of membership. More complete details on this procedure can be found in previous papers (31,32). In this case, tissues from measurement sites were classified only as normal/negative or tumor/positive because to the surgeon, knowing whether the tissue is something that should be removed is sufficient. Also, due to the nature of patients undergoing partial or total mastectomies, no measurements of benign tumors or other such conditions were possible. Since the excised tissues were only sampled in a limited manner, analysis of margin status was limited to only those points directly sampled by the probe.

The spectral images were corrected for sensitivity of the detector and transmission of the LCTF, as well as for the line shape of illumination in the case of reflectance images. Fluorescence images were binned over a 2 by 2 pixel area to account for the weaker nature of fluorescence. To display individual spectra from a point on the image, the spectra from a 20 by 20 pixel area were averaged to match the size of the optical fiber probe. No quantitative analysis was done with the images since they were a test of feasibility and there were too few of them.

3. RESULTS

Mean, normalized autofluorescence and diffuse reflectance spectra, plus and minus one standard deviation for normal tissue / negative margins (n = 145) and tumor tissue / positive margins (n = 34) from 32 patients are shown in Figures 1A and 1B, respectively. The fluorescence spectra in Figure 1A show a variety of differences between normal and tumor tissues, notably a relatively more intense peak around 390 nm in tumor tissues compared with normal, and relatively greater contributions at wavelengths longer than about 475 nm in spectra from normal tissues. The 390 nm peak is generally attributed to collagen, while the most significant differences past ~475 nm are associated with the tail of the NADH emission spectrum, which has its peak at 450 nm, and the broad peak of flavins from about 500 to 550 nm. The reflectance spectra do not show as visually obvious significant differences between the two tissue types, as the error bars always overlap. The normal reflectance spectra show an overall higher slope, though, and in many regions, the mean of each tissue class lies outside the error bars around the other class's mean.

Table 2 shows the confusion matrix for the performance of the MRDF-SMLR algorithm for combined fluorescence and reflectance with leave-one-patient-out cross-validation on all non-chemo-treated patients. Normal tissue, indicative of negative margins, was discriminated

from tumor tissue / positive margins with 85% sensitivity and 96% specificity, or 83% positive predictive value and 97% negative predictive value, or an overall accuracy of 94%. Figure 2 shows the posterior probabilities, as determined by SMLR, of each measured spectrum belonging to its true class, as determined by histopathology. Shapes near 1.0 on the vertical axis represent spectra that were determined to have a high probability of being obtained from the correct tissue type, while those below 0.5 represent spectra that were misclassified. Most normal tissue sites were classified with high probabilities, while tumor tissue probabilities are more spread out, but are still well classified.

Figure 3 displays the mean spectra from all normal tissue sites without (n = 145) and with (n = 19) neo-adjuvant chemotherapy. The spectra from sites with NAC were excluded from the previous analysis. Although the sample size of NAC-treated normal tissues is fairly small, the spectra show a significant difference from non-NAC-treated normal tissues in the peak around 500 nm. As seen in Table 3, MRDF-SMLR was able to classify spectra according to the use of NAC with 100% sensitivity and specificity.

Figure 4A shows a sample fluorescence spectral image of breast tissue following a lumpectomy, while Figure 4B shows the corresponding reflectance spectral image. The areas marked by 1 and 2 in the images correspond to a calcified lesion "abutting the margin" and normal tissue, respectively. The normalized fluorescence and reflectance spectra obtained from averaging a 20 by 20 pixel region at the marked sites are shown in Figures 4C and 4D, respectively. These two regions were difficult to distinguish on the tissue surface with the naked eye and were only slightly easier to distinguish in Figure 4B, as evidenced by the relatively small reflectance spectral differences in Figure 4D. The same areas do show apparent fluorescence

spectral differences in Figure 4C, though, and they are easily distinguished and delineated in Figure 4A.

4. DISCUSSION

The goal of the present study was to investigate the use of combined autofluorescence and diffuse reflectance spectroscopy and spectral imaging for evaluating the status of breast surgical margins. As seen in Figure 1A, the normalized fluorescence spectra from tumor / positive margin and normal / negative margin sites show a number of differences. As previously mentioned, the most significant differences are seen at spectral regions usually associated with collagen around 390 nm, with the tail of NADH emission approaching 500 nm, and with flavins from around 500 to 550 nm. These changes are consistent with those seen in other studies (26,29,31) and result from structural and metabolic changes associated with cancer. Normalized diffuse reflectance spectra, as seen in Figure 1B, show some visual differences between normal and tumor tissues, but not as significant as for some regions of the fluorescence spectra.

As seen in Table 2, the algorithm based on MRDF and SMLR classified the combined fluorescence and reflectance spectra from non-NAC-treated tissues as normal or tumor with 85% sensitivity and 96% specificity, with an overall classification accuracy of 94%. Of the six false positive results, one measurement was taken from a margin that was deemed positive by surgical pathology, but the shave biopsy from the measurement point was determined to be normal tissue. It is possible that the sampling was slightly off, or that the measurements were sensitive to nearby disease in an area deemed histologically normal. Two false positive diagnoses were from a single very dense, collagenous normal specimen. Another false positive came from a tissue sample with a positive finding at a different margin, while the other two had no notes indicating

a possible reason for misclassification. Of the five false negatives, one measurement site had a ~1 mm layer of fat over the tumor, which is likely at or near the limit of margin size that these modalities can evaluate. No specific reasons for other misclassifications could be identified.

In terms of a clinical application, the most interesting statistic is likely negative predictive value. The surgeon would like to be confident that any diagnosis of normal or negative margins is an accurate one, and he or she is not leaving any tumor tissue in the patient. A high positive predictive value would be desirable as well to avoid unnecessary re-excisions during the operation. From this data set, the negative predictive value is 97%, and the positive predictive value is 83%. Although there were close to five times as many negative spectra as positive, predictive values often taken into account different population sizes, and the distribution of measurements in this sample set is a reasonable approximation of what might be encountered in actual medical use.

As seen in Figure 2, the MRDF-SMLR algorithm determined the class membership of normal tissues with mostly high posterior probabilities. It showed less certainty in its classification of tumor tissues, seen by the greater spread of the circles on the y-axis, but still provided strong classification overall. One strength of this analysis technique is its probabilistic nature. It can provide a surgeon with the likelihood that a given measurement site is normal, indicating negative margins, or that the site contains tumor features and therefore represents a positive margin. Although two measurements may both be classified as tumor, their actual posterior probabilities of being such could differ by up to 0.49, from 0.51 to 1.0; this kind of information would be very useful in making informed medical decisions.

A number of decisions on the treatment of the data were made in the above analysis. When both non-normalized fluorescence and reflectance spectra (not shown) are examined,

tumor tissue spectra are generally more intense across all wavelengths than normal spectra, a result which has been seen before (14). Although that information may be diagnostically useful, given the difficulty of tightly controlling the measurement environment in an operating room, we felt it prudent to normalize spectra to area under the curve rather than to an intensity standard. The classification ability of either modality by itself was not evaluated; rather, the merged spectra were used since we found in a previous study on breast tissues that doing so significantly increased classification performance over the individual modalities (31). That previous study used the same instrumentation, data processing, and data analysis procedures as this study. Further, the relative means, amount of error bar overlap between categories, etc. are similar for the two studies. On a related note, intrinsic fluorescence spectra were not extracted as part of this study. Though some studies have seen success with extracting such spectra and/or individual tissue parameters from reflectance spectra, MRDF-SMLR has achieved excellent classification results without first performing these additional mathematical procedures (31,32). It is possible, though, that performing such extractions could improve future evaluation algorithms from larger, more diverse data sets.

The classification performance presented in this paper compares favorably with other recent work on the use of combined fluorescence and reflectance for *ex vivo* breast tissue discrimination. The most recent work of Zhu and Ramanujam et. al. was able to classify malignant versus normal/benign tissues with up to 87% sensitivity, 89% specificity, and 88% overall accuracy using a support vector machine (SVM) on empirically chosen principal components, or with 89% sensitivity, specificity, and overall accuracy using a SVM on parameters extracted from the spectra with a Monte Carlo model (27). A paper by Volynskaya and Feld et. al. used a diffusion equation-based model to extract parameters that were fed into a

stepwise classification algorithm. That system classified spectra as malignant or normal/benign with 100% sensitivity and 96% specificity, as well as 91% overall accuracy, which reflects some normal and benign sites being misclassified among the three possible such categories. If only diffuse reflectance spectra were analyzed, they achieved 100% sensitivity and specificity, but with 81% overall accuracy (29).

It is difficult to truly compare the results in this paper and the two studies discussed above due to a number of factors. While all three obtain measurements shortly after excision, techniques vary between and within studies as to whether they are recorded in the operating room or after sectioning by pathology. The measurements in this paper were obtained as they would be for intraoperative margin analysis, while the others were focused on measuring specific diseased or normal areas. Slightly different wavelength ranges are used, and several physical components of the measurement systems are different among all three studies. Both above studies correct the fluorescence measurements to obtain intrinsic fluorescence spectra, while this study did not, for reasons stated above. While all three studies use some form of spectral normalization, the implementations vary. The analysis methods differ as well, both in the statistical technique and in the number of tissue categories considered. Overall, the results presented in this paper for using combined fluorescence and reflectance to distinguish between malignant and normal/benign tissues are slightly better than the same measure presented by Zhu et. al. (27) but slightly worse than those of Volynskaya et. al. (29). The reasons for this could be any of the factors discussed above. The MR DF-SMLR algorithm is the only one, to our knowledge, that displays probabilities of class membership as well.

Another interesting aspect of this study was looking at the effects of neo-adjuvant chemotherapy on measurements from normal breast tissues. No measurements from NAC-

treated tumor measurements were available because in those cases, the tumors had been significantly shrunk by the chemotherapy. Most studies exclude such data, as this paper did in above analyses, since NAC can affect the biochemistry of the tissue. As seen in Figure 3, the only area of significant difference between normalized mean spectra of normal tissues with and without NAC is a peak around 500 nm. This finding is interesting because a similar phenomenon is seen in brain tissues with radiation damage (35). No mechanism for this common finding has been proposed, but it is logical that chemotherapy and radiation could induce similar biochemical responses in tissues near tumors.

From Table 3, these spectral differences allowed perfect classification of spectra from normal tissues according to NAC treatment status. Although not shown in the table, if tumor spectra from patients not undergoing NAC were included as a third category, the 19 NAC-treated normal tissues were still classified with 100% accuracy, and no other spectra were classified as being NAC-treated. With only 19 spectra from three patients in the NAC category, these analyses were not well-powered, and from a clinical perspective, "classifying" tissues according to NAC status is not relevant since that status is know *a priori*. These analyses do show that in future development of a clinical algorithm, it is likely necessary to stratify tissue classes according to both histopathology and use of NAC since the chemotherapy alters the (normal) spectra.

This paper is the first, to our knowledge, to present wide-field fluorescence and reflectance-based spectral imaging data from *ex vivo* breast tissues. The spectral images and corresponding spectra from Figure 4 demonstrate the feasibility of this modality for evaluating the surgical margin status of a lumpectomy specimen over a large area. The images in Figure 4 are of a margin with a calcified lesion, which are typically treated as malignant, "abutting the

margin" that was very difficult to see with the naked eye. It is also somewhat difficult to see in the reflectance image in Figure 4B, but it shows up as a very distinct blue-colored region in Figure 4A, labeled with the number 1. The spectra in Figures 4C-D corresponding to that lesion and to normal, fatty tissue (the number 2) confirm that these regions have very different fluorescent properties that can be demarcated on spectral images. From this very limited data set, it appears that such spectral imaging is a good candidate for evaluating the entire surface of excised breast specimens. Clear images can be obtained for a 25 mm by 25 mm field of view in a matter of minutes, and spectra with large signal to noise ratios can be obtained by averaging the spectra from a 20 by 20 pixel (1 mm^2) area. This area is equivalent to the area interrogated by the optical fiber probe and provides more than adequate spatial resolution to the surgeon.

A major limiting factor in moving from spectroscopy to imaging is the differing lineshapes of the recorded spectra (36). Although the wavelength ranges are different, one can see that the general shapes of the fluorescence spectra from Figure 1A vs. 4C and the reflectance spectra from 1B vs. 4D are different, despite all being corrected for system responses. The fluorescence spectra in Figure 4C show the same trends relative to each other as they do in Figure 1A, although both are much less intense near 400 nm. The reflectance spectra from Figure 4D have a much higher slope compared with those from Figure 1B. Both of these observations match those seen previously (36). As a result, some kind of correction must be developed if one wishes to directly compare measurements from point spectroscopy versus imaging, or one can simply develop separate algorithms and compare the performance of the two, as was done with an analogous brain tumor demarcation study (33). Given the preliminary nature of the spectral imaging data in this study, no attempt was made to correct its spectra to match those from the fiber probe instrument.

This paper has demonstrated that fluorescence and reflectance spectroscopy can evaluate the margin status of excised breast specimens with high sensitivity and specificity. Since the penetration depth of the wavelength range used in this study is not as deep as would be desired clinically, more advanced techniques would be needed to examine margin status to a greater depth. One method to probe deeper into tissue is to physically separate the source and detector fibers to collect photons that have traveled further beneath the tissue surface after undergoing multiple scattering (37). If polarized excitation light is used, varying the relative angle of a polarizer in the detection leg can make fluorescence measurements more or less sensitive to surface vs. deeper tissue components as well (38-40). In its current form, the technique presented in this paper would still be clinically useful for the ~46 % of North American institutions that do not require negative margins > 1 mm (4). The point-based measurements allow good discrimination, and the spectral imaging cases indicate the promise of interrogating larger areas of tissue in clinically feasible times.

ACKNOWLEDGMENTS

The authors thank the surgical pathology staff at VUMC for their help. They acknowledge the aid of Elizabeth Vargis in preparing the final manuscript, and the financial support of both the NCI SPORE in Breast Cancer Pilot Project grant (5P50 CA098131-03) and a Department of Defense Breast Cancer Research Program pre-doctoral fellowship (for MDK).

REFERENCES

1. American Cancer Society. Cancer Facts and Figures 2009. Atlanta: American Cancer Society; 2009.
2. Horst KC, Smitt MC, Goffinet DR, Carlson RW. Predictors of local recurrence after breast-conservation therapy. Clin Breast Cancer 2005; 5(6):425-438.

3. Dunne C, Burke JP, Morrow M, Kell MR. Effect of margin status on local recurrence after breast conservation and radiation therapy for ductal carcinoma in situ. J Clin Oncol 2009; 27(10):1615-1620.
4. Taghian A, Mohiuddin M, Jagsi R, Goldberg S, Ceilley E, Powell S. Current perceptions regarding surgical margin status after breast-conserving therapy: results of a survey. Annals of surgery 2005; 241(4):629-639.
5. Gralow JR, Burstein HJ, Wood W, Hortobagyi GN, Gianni L, von Minckwitz G, Buzdar AU, Smith IE, Symmans WF, Singh B, Winer EP. Preoperative therapy in invasive breast cancer: pathologic assessment and systemic therapy issues in operable disease. J Clin Oncol 2008; 26(5):814-819.
6. Bafaloukos D. Neo-adjuvant therapy in breast cancer. Ann Oncol 2005; 16 Suppl 2:ii174-181.
7. Balch GC, Mithani SK, Simpson JF, Kelley MC. Accuracy of intraoperative gross examination of surgical margin status in women undergoing partial mastectomy for breast malignancy. Am Surg 2005; 71(1):22-27; discussion 27-28.
8. Cabioglu N, Hunt KK, Sahin AA, Kuerer HM, Babiera GV, Singletary SE, Whitman GJ, Ross MI, Ames FC, Feig BW, Buchholz TA, Meric-Bernstam F. Role for intraoperative margin assessment in patients undergoing breast-conserving surgery. Ann Surg Oncol 2007; 14(4):1458-1471.
9. Klimberg VS, Harms S, Korourian S. Assessing margin status. Surg Oncol 1999; 8(2):77-84.
10. Alfano RR, Tang GC, Pradhan A, Lam W, Choy DSJ, Opher E. Fluorescence-Spectra from Cancerous and Normal Human-Breast and Lung Tissues. Ieee Journal of Quantum Electronics 1987; 23(10):1806-1811.
11. Alfano RR, Pradhan A, Tang GC, Wahl SJ. Optical Spectroscopic Diagnosis of Cancer and Normal Breast Tissues. J Opt Soc Amer B (Opt Phys) 1989; 6(5):1015-1023.
12. Yang Y, Katz A, Celmer EJ, Zurawska-Szczepaniak M, Alfano RR. Fundamental differences of excitation spectrum between malignant and benign breast tissues. Photochem Photobiol 1997; 66(4):518-522.
13. Yang Y, Celmer EJ, Zurawska-Szczepaniak M, Alfano RR. Excitation spectrum of malignant and benign breast tissues: a potential optical biopsy approach. Lasers Life Sci 1997; 7:249-265.
14. Gupta PK, Majumder SK, Uppal A. Breast cancer diagnosis using N2 laser excited autofluorescence spectroscopy. Lasers Surg Med 1997; 21(5):417-422.
15. Majumder SK, Gupta PK, Jain B, Uppal A. UV excited autofluorescence spectroscopy of human breast tissues for discriminating cancerous tissue from benign tumor and normal tissue. Lasers Life Sci 1998; 8:249-264.
16. Gharekhan AH, Arora S, Mayya KBK, Panigrahi PK, Sureshkumar MB, Pradhan A. Characterizing breast cancer tissues through the spectral correlation properties of polarized fluorescence. Journal of Biomedical Optics 2008; 13(5):054063-054068.
17. Alimova A, Katz A, Sriramoju V, Budansky Y, Bykov AA, Zeylikovich R, Alfano RR. Hybrid phosphorescence and fluorescence native spectroscopy for breast cancer detection. Journal of Biomedical Optics 2007; 12(1):014004-014006.
18. Yang Y, Celmer EJ, Koutcher JA, Alfano RR. DNA and protein changes caused by disease in human breast tissues probed by the Kubelka-Munk spectral functional. Photochem Photobiol 2002; 75(6):627-632.
19. Yang Y, Celmer EJ, Koutcher JA, Alfano RR. UV reflectance spectroscopy probes DNA and protein changes in human breast tissues. J Clin Laser Med Surg 2001; 19(1):35-39.
20. Yang Y, Katz A, Celmer EJ, Zurawska-Szczepaniak M, Alfano RR. Optical spectroscopy of benign and malignant breast tissues. Lasers Life Sci 1996; 7:115-127.
21. Nair MS, Ghosh N, Raju NS, Pradhan A. Determination of optical parameters of human breast tissue from spatially resolved fluorescence: a diffusion theory model. Appl Opt 2002; 41(19):4024-4035.
22. Ghosh N, Mohanty SK, Majumder SK, Gupta PK. Measurement of optical transport properties of normal and malignant human breast tissue. Applied Optics 2001; 40(1):176-184.
23. Breslin TM, Xu F, Palmer GM, Zhu C, Gilchrist KW, Ramanujam N. Autofluorescence and diffuse reflectance properties of malignant and benign breast tissues. Ann Surg Oncol 2004; 11(1):65-70.

24. Palmer GM, Zhu C, Breslin TM, Xu F, Gilchrist KW, Ramanujam N. Comparison of multiexcitation fluorescence and diffuse reflectance spectroscopy for the diagnosis of breast cancer (March 2003). IEEE Trans Biomed Eng 2003; 50(11):1233-1242.
25. Zhu C, Palmer GM, Breslin TM, Xu F, Ramanujam N. Use of a multiseparation fiber optic probe for the optical diagnosis of breast cancer. J Biomed Opt 2005; 10(2):024032.
26. Zhu C, Palmer GM, Breslin TM, Harter J, Ramanujam N. Diagnosis of breast cancer using fluorescence and diffuse reflectance spectroscopy: a Monte-Carlo-model-based approach. J Biomed Opt 2008; 13(3):034015.
27. Zhu C, Breslin TM, Harter J, Ramanujam N. Model based and empirical spectral analysis for the diagnosis of breast cancer. Optics express 2008; 16(19):14961-14978.
28. Zhu C, Palmer GM, Breslin TM, Harter J, Ramanujam N. Diagnosis of breast cancer using diffuse reflectance spectroscopy: Comparison of a Monte Carlo versus partial least squares analysis based feature extraction technique. Lasers Surg Med 2006; 38(7):714-724.
29. Volynskaya Z, Haka AS, Bechtel KL, Fitzmaurice M, Shenk R, Wang N, Nazemi J, Dasari RR, Feld MS. Diagnosing breast cancer using diffuse reflectance spectroscopy and intrinsic fluorescence spectroscopy. Journal of Biomedical Optics 2008; 13(2):024012-024019.
30. Bigio IJ, Bown SG, Briggs G, Kelley C, Lakhani S, Pickard D, Ripley PM, Rose IG, Saunders C. Diagnosis of breast cancer using elastic-scattering spectroscopy: preliminary clinical results. J Biomed Opt 2000; 5(2):221-228.
31. Majumder SK, Keller MD, Boulos FI, Kelley MC, Mahadevan-Jansen A. Comparison of autofluorescence, diffuse reflectance, and Raman spectroscopy for breast tissue discrimination. J Biomed Opt 2008; 13(5):054009.
32. Majumder SK, Gebhart S, Johnson MD, Thompson R, Lin WC, Mahadevan-Jansen A. A probability-based spectroscopic diagnostic algorithm for simultaneous discrimination of brain tumor and tumor margins from normal brain tissue. Appl Spectrosc 2007; 61(5):548-557.
33. Gebhart SC, Thompson RC, Mahadevan-Jansen A. Liquid-crystal tunable filter spectral imaging for brain tumor demarcation. Appl Opt 2007; 46(10):1896-1910.
34. Lin WC, Toms SA, Johnson M, Jansen ED, Mahadevan-Jansen A. In vivo brain tumor demarcation using optical spectroscopy. Photochem Photobiol 2001; 73(4):396-402.
35. Lin WC, Mahadevan-Jansen A, Johnson MD, Weil RJ, Toms SA. In vivo optical spectroscopy detects radiation damage in brain tissue. Neurosurgery 2005; 57(3):518-525; discussion 518-525.
36. Gebhart SC, Majumder SK, Mahadevan-Jansen A. Comparison of spectral variation from spectroscopy to spectral imaging. Appl Opt 2007; 46(8):1343-1360.
37. Keller MD, Majumder SK, Mahadevan-Jansen A. Spatially offset Raman spectroscopy of layered soft tissues. Opt Lett 2009; 34(7):926-928.
38. Ghosh N, Majumder SK, Patel HS, Gupta PK. Depth-resolved fluorescence measurement in a layered turbid medium by polarized fluorescence spectroscopy. Opt Lett 2005; 30(2):162-164.
39. Yaroslavsky AN, Salomatina EV, Neel V, Anderson R, Flotte T. Fluorescence polarization of tetracycline derivatives as a technique for mapping nonmelanoma skin cancers. Journal of biomedical optics 2007; 12(1):014005.
40. Roblyer D, Richards-Kortum R, Sokolov K, El-Naggar AK, Williams MD, Kurachi C, Gillenwater AM. Multispectral optical imaging device for in vivo detection of oral neoplasia. Journal of biomedical optics 2008; 13(2):024019.

Table 1. Breakdown of measurements by tissue types and by numbers of patients.

Tissue Category	**Number of Spectra**	**Number of Patients**
Normal 145		28
Tumor (IDC, DCIS)	34	12

Table 2. Confusion matrix for classification of non-chemo-treated tissues only.

		Spectral Classification		
		Normal Tu	mor	
Histopathology	Normal 139		6	Specificity: 96%
Diagnosis	Tumor 5		29	Sensitivity: 85%
		NPV: 97%	PPV: 83%	

Table 3. Confusion matrix for classifying all normal tissues according to the use of neo-adjuvant chemotherapy.

		Spectral Classification	
		No Chemo	Neo-adjuvant Chemo
Chemotherapy Status	No Chemo	145	0
	Neo-adjuvant Chemo	0	19

Figure 1. Mean, normalized (A) autofluorescence and (B) diffuse reflectance spectra for patients not receiving any neo-adjuvant chemotherapy. Error bars represent one standard deviation.

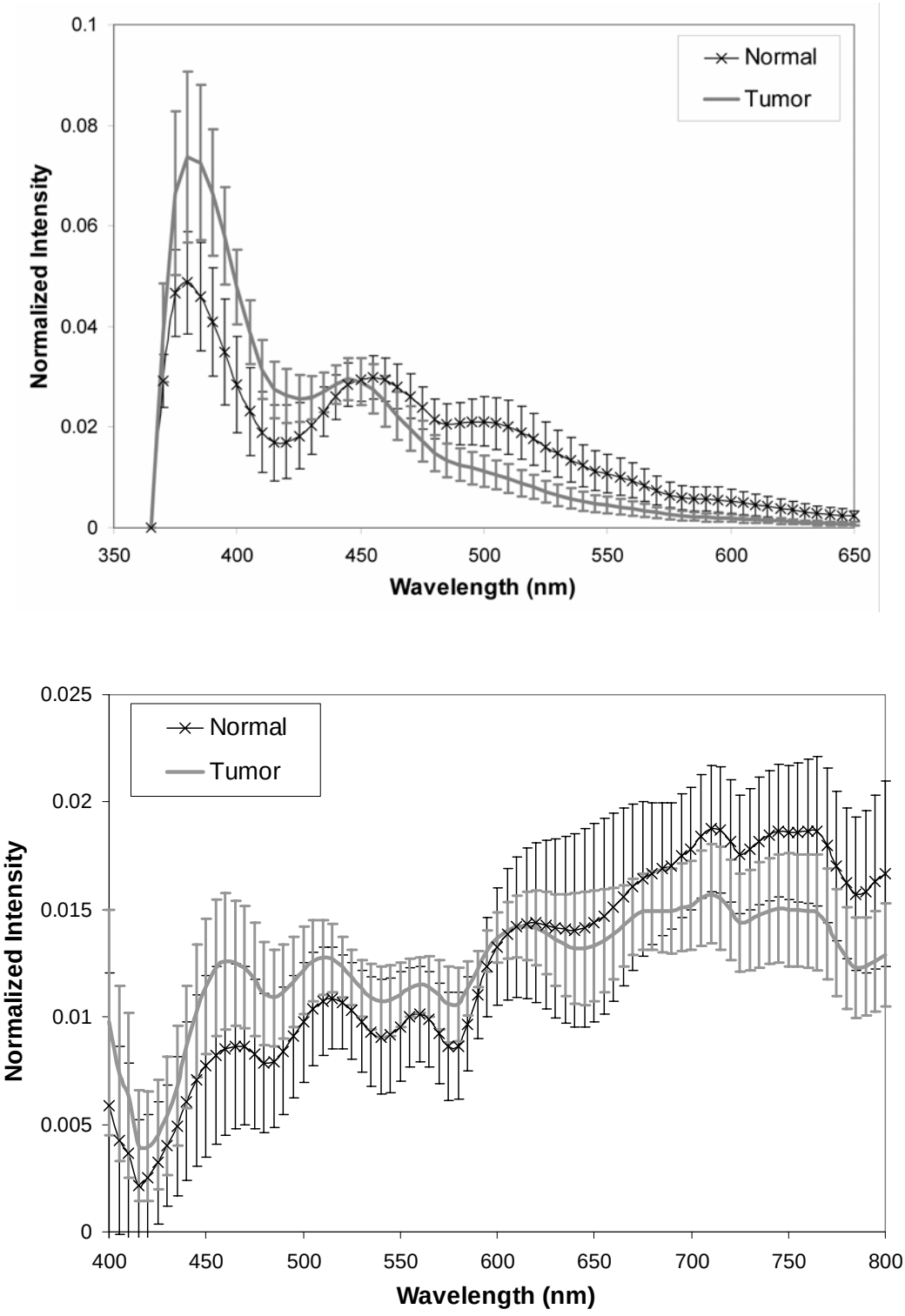

Figure 2. Results of SMLR classification. Each symbol denotes an interrogated tissue site (squares for histopathologically normal, circles for tumor), with their associated probabilities of belonging to their true tissue class according to the spectral classification.

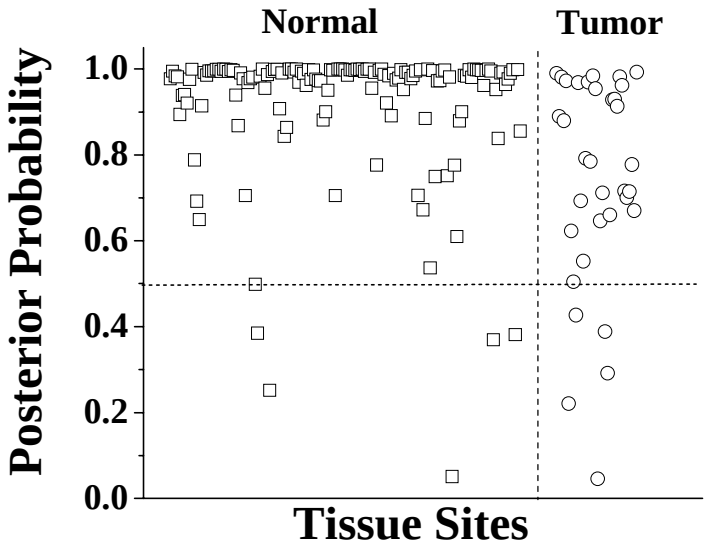

Figure 3. Mean, normalized autofluorescence spectra, plus or minus one standard deviation, for normal tissue measurements with and without neo-adjuvant chemotherapy.

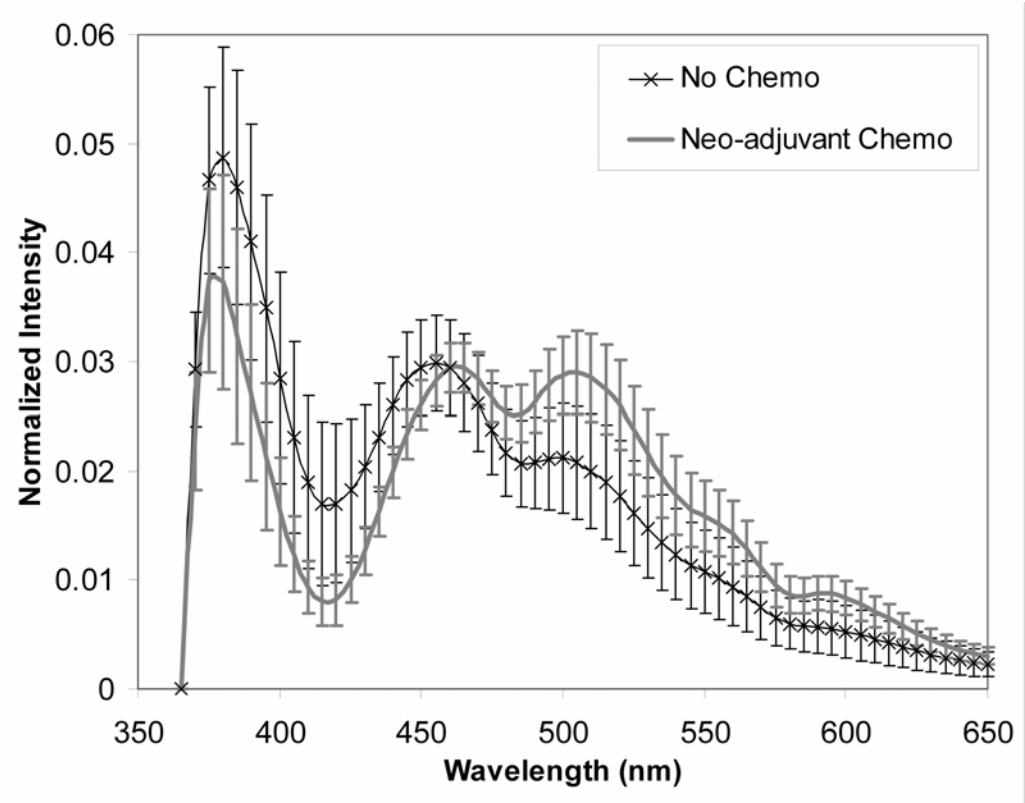

Figure 4. Spectral images and selected spectra from a lumpectomy specimen. (A) Fluorescence spectral image. (B) Diffuse reflectance spectral image. (C) Fluorescence and (D) diffuse reflectance spectra corresponding to points 1 and 2 in (A) and (B), respectively.

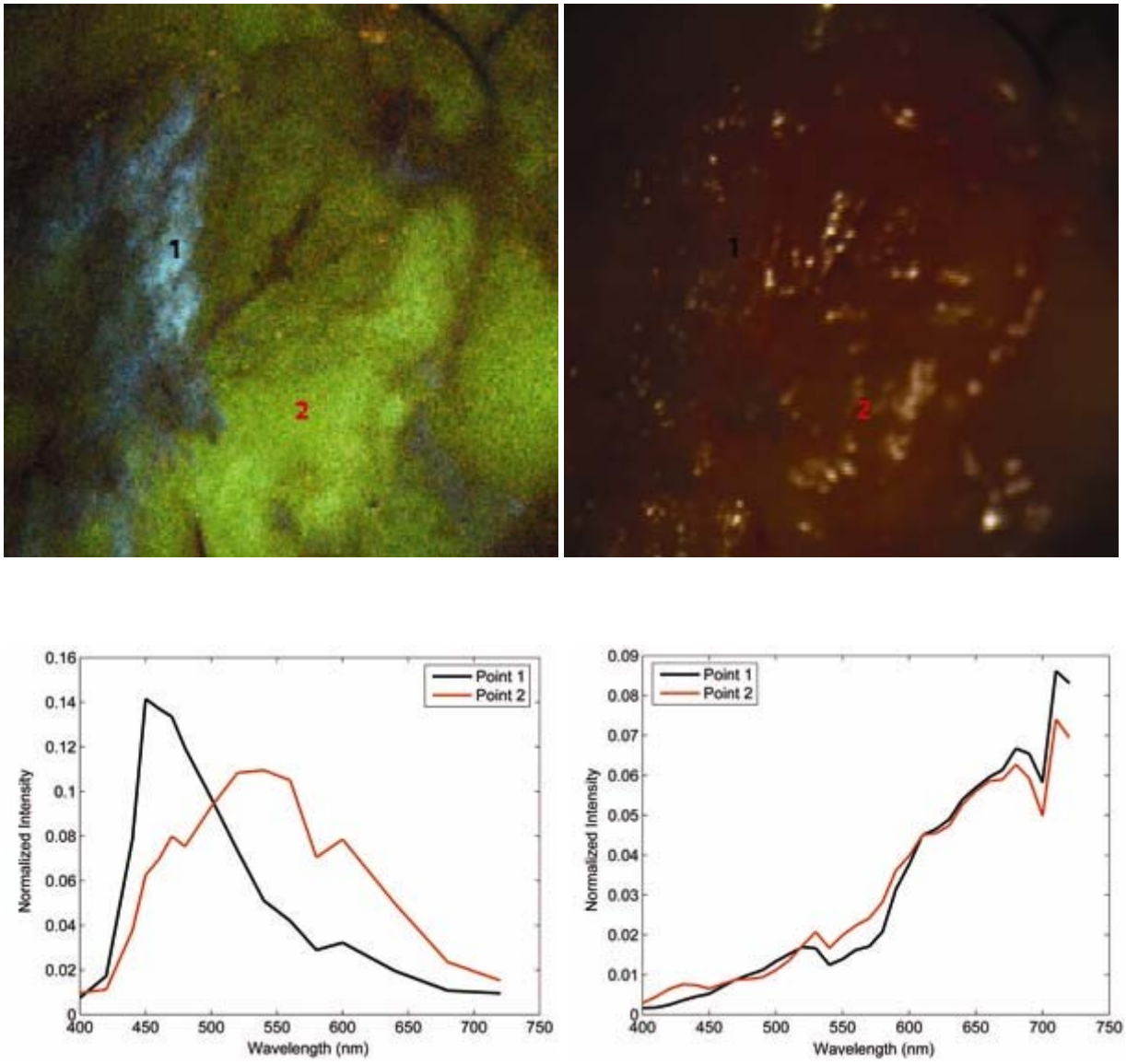

Spatially offset Raman spectroscopy of layered soft tissues

Matthew D. Keller[1] and Anita Mahadevan-Jansen[1*]

[1]*Biomedical Engineering Department, Vanderbilt University, VU Station B 351631, Nashville, TN 37235, USA*

[*]*Corresponding author: anita.mahadevan-jansen@vanderbilt.edu*

Raman spectroscopy has been widely used fo r cancer diagnosis, but conventional for ms provide limited depth infor mation. Spatially offset Raman spectroscopy (SORS) can solve the depth issue, but it has only b een used to detect hard tissues like bone. The feasibility of using SORS to discrim inate two layers of soft tissu e is explor ed in this letter . Measurements were taken with individual source and detector fibers at a num ber of spatial offsets from sam ples consisting of various thicknesses of norm al hu man breast tissues overlying breast tumors. Results show that SORS can detect tumors beneath normal tissue, marking the first application of SORS for disc riminating two layers of soft tissue.

OCIS codes: 170.5660, 170.4580, 170.6510, 170.4730, 170.3660

Several groups have successfully applied Raman spectroscopy for cancer diagnosis, primarily in epithelial tissues [1] because of the limited depth from which typical Raman setups can gather significant signal. The most practical and promising method for detecting signals from deeper tissues, at least 1 mm below the surface, is introducing a spatial offset between the delivery and collection fibers in a technique known as spatially offset Raman spectroscopy (SORS) [2].

In SORS, larger offsets are more likely to detect photons that have traveled deeper into tissue via multiple scattering, compared with smaller separations, which detect superficial photons that have only undergone minimal scattering events. Matousek et al. first demonstrated SORS of diffusely scattering media using a two-layer chemical phantom [2]. To date, the primary biological application of this technique has been detecting the strong Raman signature of bone through several mm of soft tissue [3-5]. It has also been used to detect the Raman spectral features of hydroxyapatite crystals (found in breast calcifications) through overlying lean chicken breast tissue [6]. Thus, the application of SORS has been limited to detecting very strong scatterers with unique spectral features under a layer of generic soft tissue. No work has, to our knowledge, yet been published in applying SORS to discriminating multiple layers of soft tissue.

One relevant application of using SORS for soft tissues would be evaluating margin status during breast conserving therapy (BCT). This process involves a lumpectomy for the removal of the primary breast lesion, usually followed by radiotherapy. To be successful, BCT must provide negative margins, meaning there is no presence of tumor in the removed tissue within 1-2 mm (depending on hospital) of the surgical margin [7]. The definitive diagnosis of margin status is provided by serial sectioning with histopathology, but results are slow, and current intraoperative techniques all have limitations in accuracy and/or time required [8].

A recent review of the use of Raman spectroscopy for breast cancer diagnosis was offered by Krishna et al. [9]. We have also conducted a recent study in which nearly 300 Raman spectra from *in vitro* breast samples were classified into four histopathological categories with 99% overall accuracy [10]. It should be noted that the vast majority of the published work is focused on diagnosis of breast cancer and not for guidance of therapy or margin assessment. Additionally, no published work considers the need for determining margin status to a depth of 1-2 mm on the excised specimen.

Besides the general purpose of demonstrating the use of SORS in soft tissues, the goal of this study was to assess the feasibility of using SORS to detect the Raman signatures of breast tumors beneath relevant thicknesses of normal breast tissue to mimic the clinical situation of evaluating margin status. A schematic of the experimental setup used is shown in Fig. 1. Layers of normal human breast tissue, which consisted of mostly adipose with some fibroglandular tissue, were sealed between two ~100 μm thick quartz coverslips to prevent dehydration and to minimize the impact of non-biological materials on the results. Normal layer thicknesses of 0.5, 1, and 2 mm were achieved by placing appropriate spacers between the coverslips. These thicknesses were chosen to represent the clinical margin standards and to include a thinner layer as a positive control. These normal layers were placed directly on top of invasive breast cancer tissue samples, which ranged from ~2-5 mm thick, obtained fresh-frozen from the Cooperative Human Tissue Network and thawed at room temperature in buffered saline. In all, three tumor samples were used, while two normal tissue samples were used to create the normal layers.

SORS measurements were taken with single 200 μm excitation and collection fibers, featuring in-line bandpass and longpass filters, respectively, at their tips (Emvision, Loxahatchee, FL). The source fiber was fixed in place and delivered 80 mW of power from a

785 nm diode laser (Innovative Photonics Solutions, Monmouth Junction, NJ). The collection fiber was able to translate in a straight line and delivered light to the detection elements: an imaging spectrograph (Kaiser Optical Systems, Inc., Ann Arbor, MI) and a back illuminated, deep depletion, thermo-electrically cooled charge coupled device camera (Andor Technology, Belfast, Northern Ireland). Measurements were taken with spatial offsets from 0.75 to 4.75 mm in 0.5 mm intervals. For each offset, two 30 second integrations were acquired and averaged before further analysis. To achieve a smaller offset and as a point of comparison, spectra were also obtained with the same instrumentation but with a more standard fiber optic probe with a central 400 μm delivery fiber and seven surrounding 300 μm collection fibers, all featuring in-line filtering at their tips (Emvision). All seven fibers were binned after a single 3 second acquisition, and these measurements were considered to be taken with a 0.35 mm source-detector offset. All spectra were calibrated, noise smoothed, and had background fluorescence subtracted as previously described [11]. Normalization was achieved by dividing each processed spectrum by its overall mean intensity.

Figure 2 shows a sample of spectra obtained from a single experimental run with a 0.5 mm normal layer over an invasive cancer tissue sample, as well as the mean spectra from the individual normal and tumor layers. From a visual inspection, it is clear that as spatial offset increases, the spectra begin to increasingly resemble the tumor spectrum compared with the normal spectrum. The light gray boxes in Fig. 2 highlight the spectral regions subject to the most dramatic changes as spatial offset increases. These include the increased presence of the 1006 cm^{-1} peak generally attributed to phenylalanine; a decreasing ratio of the 1303 cm^{-1} to 1265 cm^{-1} peaks, which tends to indicate an increasing protein content; and the increasing width of the amide I peak around 1656 cm^{-1}. Another significant change that is somewhat difficult to

appreciate in Fig. 2 is a decrease in the relative intensity of the 1445 cm^{-1} CH_2 deformation peak as spatial offset increases, while other subtle changes include a decrease in the 1748 cm^{-1} carbonyl stretch peak and an increase in the 1156 cm^{-1} carotenoid peak as offset increases.

The results of this study were quantified by developing a classical least squares (CLS) model via the PLS_toolbox (Eigenvector Research, Wenatchee, WA) within a MATLAB (Mathworks, Natick, MA) environment. Five Raman measurements from each normal tissue layer only were averaged together, and five measurements from each tumor sample only were averaged; these two means were then used as pure component spectral inputs to create a CLS model. This model was subsequently applied to the spectra collected from each spatial offset to determine the relative contributions of the normal and tumor spectral signatures to the offset spectra. These two relative contributions always sum to 1, and the model was constrained to fitting the data in a non-negative manner. The relative tumor contributions were then averaged across the three experimental runs for analysis.

Figures 3 and 4 show the results of the CLS analysis in complementary fashion. Both plot the relative tumor spectrum contributions to the offset spectra on the y axis, but Fig. 3 shows how this metric changes as a function of source-detector offset for the three different normal layer thicknesses, while Fig. 4 displays it as a function of normal layer thickness for a range of spatial offsets. Most generally, both figures quantitatively support the visual evidence from Fig. 2 that SORS can indeed detect Raman spectral contributions from breast tumors beneath the relevant depths of normal tissue that standard configurations (0.35 mm offset) cannot. From Fig. 3, this effect follows a quadratic- or logarithmic-shaped response as spatial offset increases, and it seems to indicate that for this tissue system, S-D offsets of more than about 4 mm do not provide any additional useful information. An interesting effect is shown most explicitly in Fig.

4, which shows that as the normal layer thickness increases, there is a tighter grouping of data points along the y axis. This trend hints at a maximum top layer thickness that would allow detection of the bottom layer, which is likely limited by the achievable signal to noise ratio of the bottom layer and the absolute signal strength compared with the top layer.

The findings of this letter have some key similarities to and differences from previous SORS studies. The shapes of the responses to changes in spatial offset and top layer thickness in Figs. 3 and 4, respectively, match up well with similar plots in earlier studies [2,5]. Unlike earlier reports, in which the spectrum of the bottom layer contained strong, unique bands, these trends were observed with two layers of soft tissue whose Raman spectra differ in a subtle manner. This limits, or at least severely complicates, the use of some analytical techniques used in other SORS studies. A simple, two component CLS model with a direct physical basis worked well for validating the application of SORS to soft tissues, although a more complex model or an entirely different method of analysis may be more appropriate for clinical applications.

A number of other issues will need to be addressed to move from this proof of principle experiment toward a clinical application. The variability within these measurements will need to be considered, particularly as it relates to tissue composition, since some of the "noise" in Figs. 3 and 4 is likely due to tissue heterogeneities. While no obvious Raman signal from the coverslips was observed, their inclusion provided an unnatural discontinuity between tissue types. Based on previous measurements from a layered tissue model without using coverslips (unpublished), their presence did not seem to induce any spectral effects, so their ability to precisely control layer thickness outweighed other potential negatives at this stage. Given that tumors generally do not actually have planar boundaries, identifying the detection limit for finding small pockets of cancer cells or micro-invasions becomes important. Since the smallest portion of a tumor sample

used in this study was around 1-2 mm thick, it is difficult to speculate on the minimum number of tumor cells that could be detected. Based on trends in Figs. 3 and 4, though, it appears likely that cancerous regions smaller than those used in this study could be detected under at least a 1 mm overlying layer. This issue of detection limits will be a focus of future research, which includes the development of suitable numerical simulations with a Monte Carlo model. While Raman tomography would also theoretically be a good tool to limit the negative effects of photon diffusion on finding small pockets, its resolution is currently too poor without the aid of spatial priors [12], which would be impractical to obtain for a BCT application.

This letter has demonstrated that SORS can detect the spectral signatures of breast tumors as small as 1-2 mm thick under up to 2 mm of normal breast tissue. Although a number of questions about its efficacy require further study, this report shows that SORS of soft tissues likely holds promise for biomedical applications previously considered "out of reach" for Raman spectroscopy.

The authors acknowledge the financial support of the US Department of Defense Breast Cancer Research Program.

References

1. M. D. Keller, E. M. Kanter, and A. Mahadevan-Jansen, "Raman spectroscopy for cancer diagnosis," Spectroscopy **21**, 33-41 (2006).

2. P. Matousek, I. P. Clark, E. R. Draper, M. D. Morris, A. E. Goodship, N. Everall, M. Towrie, W. F. Finney, and A. W. Parker, "Subsurface probing in diffusely scattering media using spatially offset Raman spectroscopy," Appl Spectrosc **59**, 393-400 (2005).

3. P. Matousek, E. R. Draper, A. E. Goodship, I. P. Clark, K. L. Ronayne, and A. W. Parker, "Noninvasive Raman spectroscopy of human tissue in vivo," Appl Spectrosc **60**, 758-763 (2006).

4. M. V. Schulmerich, K. A. Dooley, M. D. Morris, T. M. Vanasse, and S. A. Goldstein, "Transcutaneous fiber optic Raman spectroscopy of bone using annular illumination and a circular array of collection fibers," Journal of biomedical optics **11**, 060502 (2006).

5. N. A. Macleod, A. Goodship, A. W. Parker, and P. Matousek, "Prediction of sublayer depth in turbid media using spatially offset Raman spectroscopy," Analytical chemistry **80**, 8146-8152 (2008).

6. N. Stone, R. Baker, K. Rogers, A. W. Parker, and P. Matousek, "Subsurface probing of calcifications with spatially offset Raman spectroscopy (SORS): future possibilities for the diagnosis of breast cancer," Analyst **132**, 899-905 (2007).

7. K. C. Horst, M. C. Smitt, D. R. Goffinet, and R. W. Carlson, "Predictors of local recurrence after breast-conservation therapy," Clin Breast Cancer **5**, 425-438 (2005).

8. N. Cabioglu, K. K. Hunt, A. A. Sahin, H. M. Kuerer, G. V. Babiera, S. E. Singletary, G. J. Whitman, M. I. Ross, F. C. Ames, B. W. Feig, T. A. Buchholz, and F. Meric-Bernstam, "Role for intraoperative margin assessment in patients undergoing breast-conserving surgery," Ann Surg Oncol **14**, 1458-1471 (2007).

9. C. M. Krishna, J. Kurien, S. Mathew, L. Rao, K. Maheedhar, K. K. Kumar, and M. Chowdary, "Raman spectroscopy of breast tissues," Expert Rev Mol Diagn **8**, 149-166 (2008).

10. S. K. Majumder, M. D. Keller, M. C. Kelley, F. I. Boulos, and A. Mahadevan-Jansen, "Comparison of autofluorescence, diffuse reflectance, and Raman spectroscopy for breast tissue discrimination.," J Biomed Optics **13**, 054009 (2008).

11. C. A. Lieber and A. Mahadevan-Jansen, "Automated method for subtraction of fluorescence from biological Raman spectra," Appl Spectrosc **57**, 1363-1367 (2003).

12. S. Srinivasan, M. Schulmerich, J. H. Cole, K. A. Dooley, J. M. Kreider, B. W. Pogue, M. D. Morris, and S. A. Goldstein, "Image-guided Raman spectroscopic recovery of canine cortical bone contrast in situ," Optics express **16**, 12190-12200 (2008).

Figure Captions

Fig. 1. Schematic of experimental setup. Normal breast tissue thicknesses of 0.5, 1, and 2 mm were used.

Fig. 2. Raman spectra from an experimental run with a 0.5 mm normal layer. Gray boxes highlight regions with most dramatic changes from normal to tumor signatures as source-detector offset (labeled on left) increases.

Fig. 3. Mean relative contributions of the Raman tumor signature to the measured spectra at each source-detector offset for the various thicknesses of the normal tissue layer. Error bars represent standard error.

Fig. 4. Same data from Fig. 3, but shown as function of normal layer thickness for selected S-D separations.

Fig 1

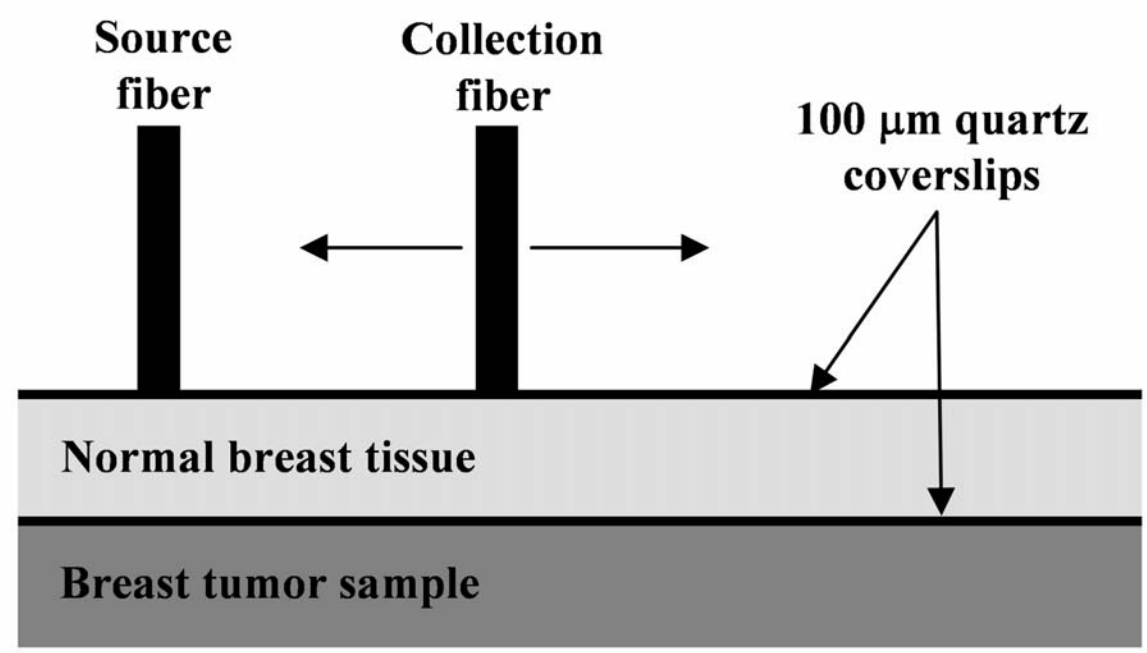
Source fiber
Collection fiber
100 μm quartz coverslips
Normal breast tissue
Breast tumor sample

Fig 2

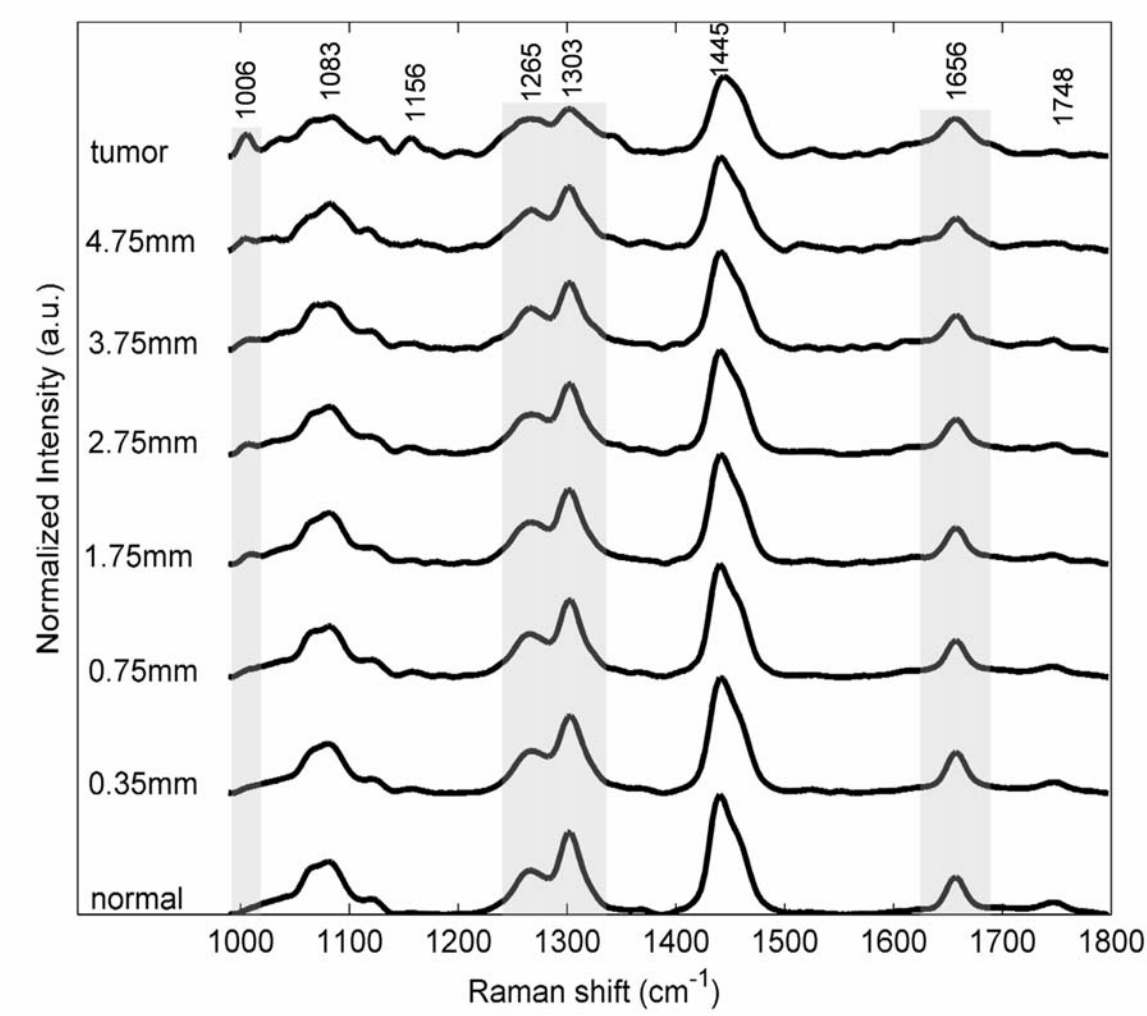
1006
1083
1156
1265
1303
1445
1656
1748
tumor
4.75mm
3.75mm
2.75mm
1.75mm
0.75mm
0.35mm
normal
Normalized Intensity (a.u.)
1000
1100
1200
1300
1400
1500
1600
1700
1800
Raman shift (cm-1)

Fig 3

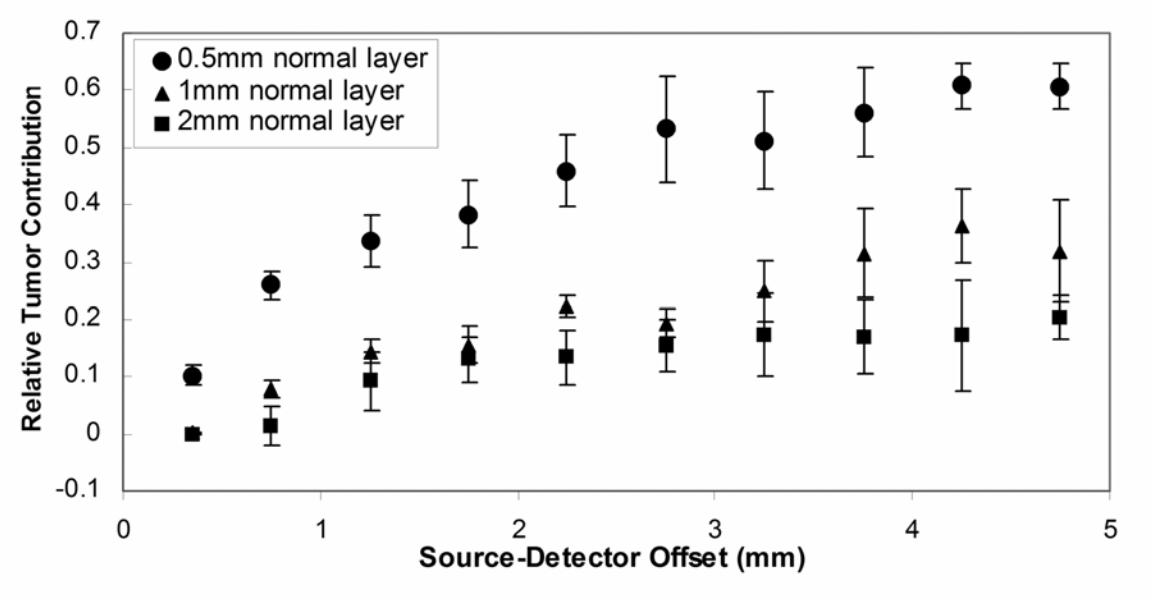
0.5mm normal layer
1mm normal layer
2mm normal layer
Relative Tumor Contribution
0.7
0.6
0.5
0.4
0.3
0.2
0.1
0
-0.1
0
1
2
3
4
5
Source-Detector Offset (mm)

Fig 4

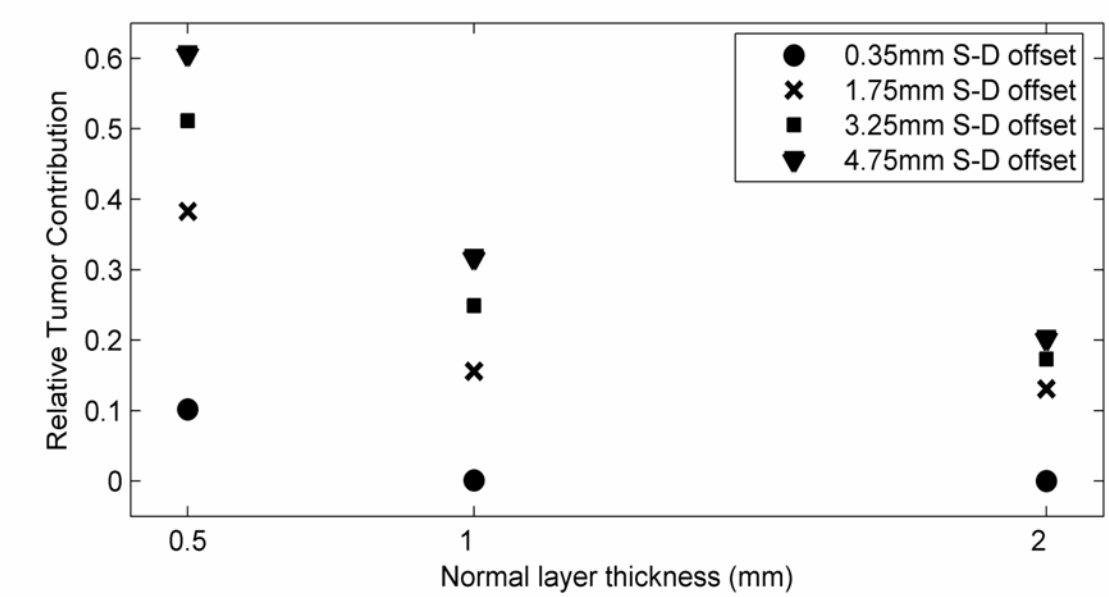
0.35mm S-D offset
1.75mm S-D offset
3.25mm S-D offset
4.75mm S-D offset
Relative Tumor Contribution
0.6
0.5
0.4
0.3
0.2
0.1
0
0.5
1
2
Normal layer thickness (mm)